results in up-field shifts of the two urea protons to similar degrees, supporting this proposal. The gas-phase DFT studies underscored the results of the NMR measurements, even though the computed structure of the catalyst–product complex only provided one hydrogen bond as the most energetically favorable complex. The bridging interaction in the catalyst–substrate complex was found stronger (8.5 kcal $mol^{-1}$ for urea; 10.0 kcal $mol^{-1}$ for thiourea) than the single hydrogen bond event (5.0 and 6.3 kcal $mol^{-1}$, respectively). Based on these results, the authors describe the reversible formation of an imine–catalyst complex with **182** binding the imine through hydrogen bonding (cf. Scheme 1.8), with approximately 80% formation of the complex found in NMR experiments. Furthermore, the model of the catalyst–substrate complex provided information about the observed scope and stereoselectivity of the Schiff base (thio)urea-catalyzed Strecker reaction:

(1) The large group on the imine carbon is directed away from the catalyst and into the solvent. This explains why the Schiff base catalyst promoted hydrocyanations with high *ee*-values, regardless of the steric and electronic properties of the substrate.
(2) The small group (H for aldimines and Me for methylketoimines) is directed toward the catalyst, which indicates that ketoimines bearing larger substituents are poor substrates for the reaction, presumably because they could not adopt the optimal geometry.
(3) The N-substituent is also directed away from the catalyst. However, its size is restricted as a result of the requirement to access the *Z*-isomer of the imine.
(4) On the basis of the observed trend of stereoinduction, addition of HCN takes place over the diaminocyclohexane portion of the catalyst and away from the amino acid/amide portion.

Following the work of Kotke and Schreiner in anion-binding catalysis in 2006 (cf. Schemes 1.12 and 1.13 [176]), Zuend and Jacobsen re-examined the cyanide addition to imines utilizing computations, Hammett analyses, catalyst structure/activity relationships, and isotope labeling studies and concluded that non-covalent interactions are crucial for stereoinduction [184]. The authors utilized modified (thio)urea derivatives of catalyst **182** and instead of the diaminocyclohexane moiety various phenyl substituents were incorporated, especially the well-established 3,5-bis(trifluoromethyl)phenyl group [190]. Similar to the work of Vachal and Jacobsen in 2002, Zuend and Jacobsen observed first-order kinetics for imine and HCN; however, the value of 0.8 for the catalyst is different from the previous work utilizing **182** (*vide supra*). Utilizing "same excess" experiments, the authors excluded deactivation of the catalyst and that product inhibition was negligible. After the authors excluded the competitive uncatalyzed background reaction due to the high *ee*-values and the slow initial rate of approximately 5% compared to the catalyzed reaction, they proposed a small degree of catalyst dimerization that was also observed in previous work [353, 354]. A Hammett analysis for distinguishing the two possible reaction pathways that could be started by protonation of the imine (Scheme 1.41a) or by addition of cyanide to the imine (Scheme 1.41b) provided strong evidence for the former because negative $\rho$-values were obtained

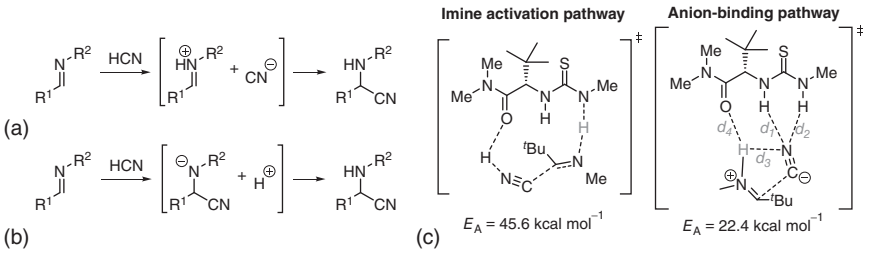


**Scheme 1.41** Two possible mechanistic pathways of (thio)urea-catalyzed Strecker reaction *via* (a) an iminium ion or (b) an α-aminonitrile anion and (c) computed activation energies for both reaction pathways.

($\rho_{\text{thiourea}} = -2.7$; $\rho_{\text{urea}} = -2.5$). Additionally, utilizing uncorrected DFT gas-phase computations (B3LYP/6-31G(d)) on a reduced model system (cf. Scheme 1.41c) at 0 K, the authors found that the activation barrier for the iminium activation pathway was approximately 23 kcal mol$^{-1}$ higher in energy than the anion-binding pathway and that the activation energy using urea catalyst is about 5.6 kcal mol$^{-1}$ higher than that of the thiourea catalyst [184].

Based on these result, Zuend and Jacobsen investigated a mechanism based on the thiourea binding the cyanide and forming an ion pair complex with the iminium ion utilizing isotope labeling experiments [184]. The authors utilized DCN and obtained the N-deuterated Strecker product, which indicated that the N–H protons of the (thio)urea moiety do not acts as Brønsted acids as would be required in pathway **B** (Scheme 1.41c). Based on the computations noted above, the authors proposed a reaction pathway that includes proton transfer of HCN (or HNC) to the imine, and generation of a thiourea-bound cyanide–iminium ion pair (Scheme 1.41c). The experimental energy differences ($\Delta G$) between the HCN and HNC protonation pathways were too low to be distinguished. Nevertheless, the outcome is the same, as the HNC protonation pathway convert into the HCN protonation pathway because of rearrangement of the cyanide ion during the reaction. This proposed mechanism was supported by the strong correlation between the experimental and the computed enantioselectivities for eight different thiourea catalysts. To elucidate the stereoinduction, correlation plots were constructed for different bond lengths vs. enantioselectivity. No trend was observed when plotting the sum of the computed thiourea–cyanide bond lengths ($d_1 + d_2$) vs. enantioselectivity, implying that the enantioselectivity cannot result from the stabilization of the cyanide. In contrast, a positive correlation was observed between the enantioselectivities and the computed imine N–H hydrogen bond distances to the cyanide anion and amide carbonyl ($d_3 + d_4$) (Scheme 1.41c). Therefore, the enantioselectivity can be ascribed to the stabilization of the iminium cation in the diastereomeric transition states of the ion pair rearrangement [184]. All in all, the authors showed that secondary design elements for the formation of NCIs are crucial for stereoinduction. Simultaneously, Jacobsen's group utilized thiourea **183** (2 mol%) in Strecker reactions of various imines and obtained the products **185** in yields ranging from 96% to 99% and *ee*-values of 73% to 99% [355]. Compared to the previously utilized Schiff base **182**,

the catalyst loading was slightly higher, but the yields and *ee*-values significantly increased. The authors developed two different methods for the *in situ* generation of HCN utilizing KCN + AcOH or TMSCN + MeOH. The KCN/AcOH method gave the products with slightly decreased enantioselectivities at higher reaction temperatures, concentrations, and reaction rates (Scheme 1.42). Additionally, solid KCN is more practical than liquid TMSCN, and starting with the imine of pivaldehyde, Jacobsen's group obtained (*R*)-Boc-*tert*-leucine in 62–65% yield of crystalline product and 98–99% *ee* over four steps [355].

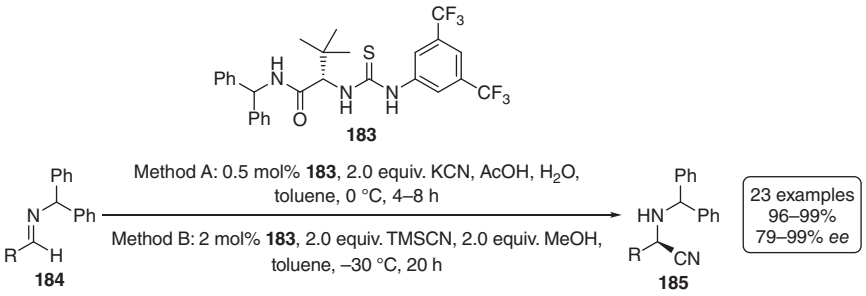


**Scheme 1.42** The improved Strecker reaction of various aldimines with thiourea **183** with two different HCN sources.

In addition to the Strecker reaction, the Michael addition is a common and often used reaction in organic synthesis [356–358]. In 2003, Takemoto and coworkers introduced bifunctional catalyst **49** for the use in this kind of addition reaction (cf. Scheme 1.11) [161]. Takemoto's group synthesized a series of diaminocyclohexane-based thioureas (e.g., **49** and **189–192**) and screened them in the model Michael addition of diethyl malonate **186** to *trans*-β-nitrostyrene **187** at room temperature (Scheme 1.43). The authors identified tertiary amine-functionalized **49** as the most efficient catalyst in terms of catalytic activity (86% yield; 24 h) and enantioinduction (83% *ee*). Utilizing the chiral amine **189** that lacks the thiourea moiety, Takemoto's group obtained **188** in only 14% yield (24 h) and 35% *ee*. With achiral **190** lacking the tertiary amine group (requiring addition of 10 mol% triethylamine), the authors provided **188** in only 57% yield after 24 h. Using bulkier tertiary amine **191** and longer reaction time (48 h), the yield decreased (76%; 48 h) and the *ee*-value was slightly lower (87%). Comparing **49** and **192**, which lacks the two $CF_3$ groups, the advantage of the 3,5-bis(trifluoromethyl)phenyl motif was well recognized [157, 158, 190], as **192** provided the Michael adduct in only 58% yield and 80% *ee* within 48 h (Scheme 1.43) [161].

In 2005, Takemoto's group investigated the mechanism of the **49**-catalyzed Michael addition utilizing NMR kinetic studies and NMR titrations and postulated a reaction mechanism that starts with the deprotonation of the C–H-acidic 1,3-dicarbonyl compound by the tertiary amine and formation of complex (**193**), in which the six-membered enol of **187** is stabilized through interactions with the protonated tertiary amine group of **54** [175]. Subsequently, thiourea's N–H protons coordinate with the Michael acceptor through hydrogen-bonding interactions

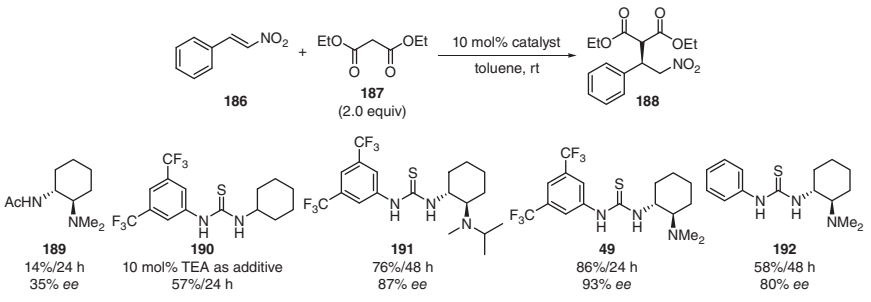


**Scheme 1.43** Catalyst screening using chiral 1,2-diaminocyclohexane **413** and various thiourea derivatives in asymmetric Michael addition of diethyl malonate to *trans*-β-nitrostyrene.

resulting in the organized ternary complex (**194**) and a relative orientation that allows nucleophilic attack in an (*R*)-favored mode leading to complex (**195**). After final protonation, the catalyst–product complex dissociates and furnishes free catalyst and **188** (Scheme 1.44). Based on this proposed mechanism, Liu and coworkers performed DFT computations (B3LYP/6-31G(d)), utilizing diethyl malonate and simplified nitroethene as well as the corresponding urea of **49**

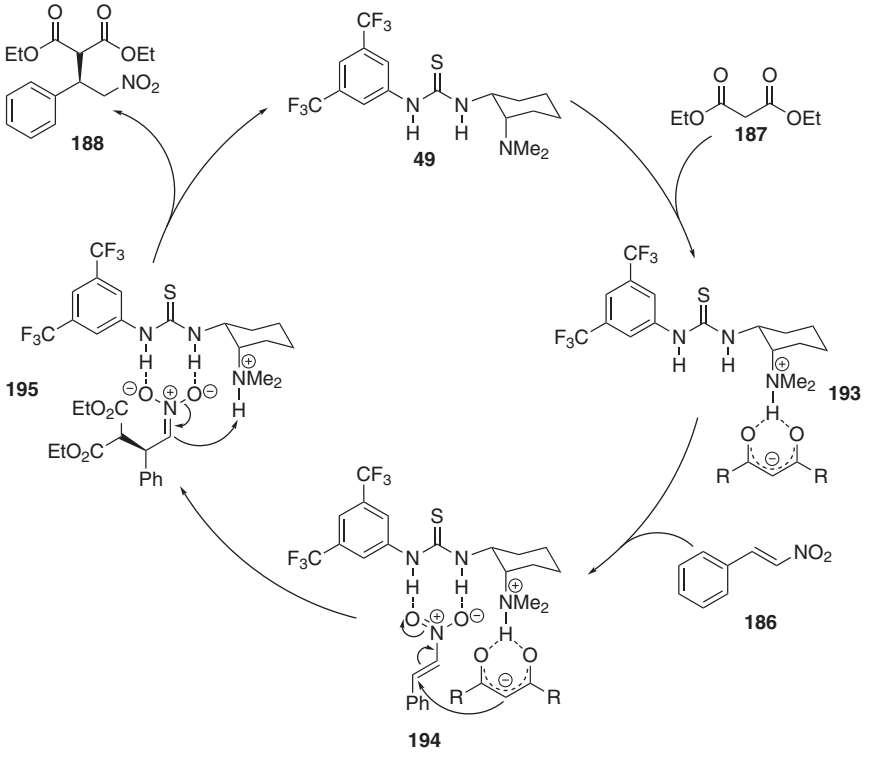


**Scheme 1.44** Postulated mechanism of the enantioselective Michael addition between *trans*-β-nitrostyrene **186** and diethyl malonate **187** promoted by bifunctional **49**.

unfortunately lacking the 3,5-bis(trifluoromethyl)phenyl substituent, and proposed that the C–C bond formation step from **194** to **195** is enantiodetermining, while the reprotonation from catalyst's amine to the α-carbon in complex **195** was identified as the rate-determining step [359].

In the following years, thiourea **49** and its derivatives were well established in organic synthesis and were utilized in many asymmetric reactions [4, 360–363]. The synergetic activation of nucleophile and electrophile, leading to high conversion and enantioselectivity, was generally accepted. In 2006, Soós, Pápai, and coworkers reinvestigated the mechanism of the **49**-catalyzed Michael addition utilizing DFT methods (B3LYP/6-311++G(d,p)//B3LYP/6-31G(d)), with β-nitrostyrene as Michael acceptor and 2,4-pentadienone as Michael donor [364]. The authors investigated in addition to Takemoto's mechanism (hydrogen-bonding activation; pathway A) an alternative mechanism *via* anion binding of the enolate (pathway B). Both mechanisms afford the (*R*)-configured product; nevertheless, the transition structure for pathway B is preferred by $\Delta\Delta G = 2.7\,\mathrm{kcal\,mol^{-1}}$ compared to pathway A because of the higher number of NCIs. This theoretical study reveals the alternative mechanism of the **49**-catalyzed Michael addition and provides strong evidence for the anion-binding mode. In 2019, Hirschi, Vetticatt, and coworkers utilized a combination of experimental $^{13}C$ kinetic isotope effects (KIEs) and DFT computations (B3LYP/6-31+G(d,p)/PCM (toluene)) for mechanistic investigations on the **49**-catalyzed Michael addition of diethyl malonate to β-nitrostyrene [365]. The authors found the lowest lying transition structure **196**, which is very similar to that described in previous work [366]. Moreover, the lowest lying transition structure **197** of the opposite enantiomer was $\Delta\Delta G = 2.4\,\mathrm{kcal\,mol^{-1}}$ higher in energy because of the lack of the stabilizing hydrogen bond between the ortho C–H and the carbonyl oxygen. Furthermore, a similar transition structure **198** to that postulated by Takemoto's group (hydrogen bond activation of the nitroolefin) [175], but incorporating an additional hydrogen bond between ortho C–H and the carbonyl oxygen, was computed and found to be $\Delta\Delta G = 4.7\,\mathrm{kcal\,mol^{-1}}$ higher in energy (Scheme 1.45). The authors also computed the transition structures for the deprotonation of the diethyl malonate and the reprotonation of the nitronate, and the corresponding KIEs for the key carbon atoms of the reactants for all computed transition structures. The authors found that the C–C bond forming step is the rate-determining as well as the enantiodetermining step of this reaction, which was inconsistent to the proposed mechanism by Liu and coworkers [359], who postulated the reprotonation of the nitronate as the rate-determining step. The work by Hirschi, Vetticatt, and coworkers confirmed the anion-binding mode of the **49**-catalyzed Michael addition.

### 1.2.3 Anion-Binding Catalysis in Substitution Reactions

(Thio)ureas are well known as potent halide-binding hosts in supramolecular chemistry, and the corresponding supramolecular complexes could be easily investigated *via* $^{1}H$ NMR and IR spectroscopy [82, 367]. Therefore, over the years, many halide-binding approaches utilizing (thio)ureas were developed, in particular,

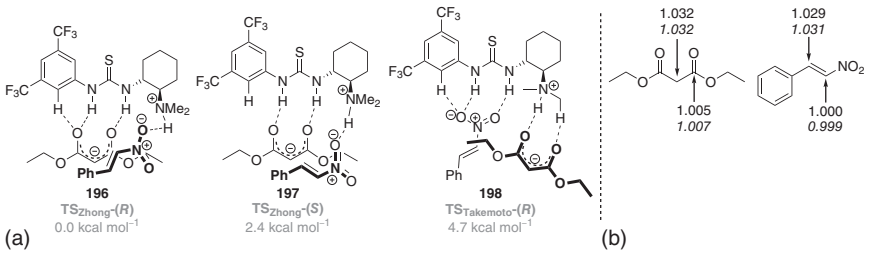


**Scheme 1.45** (a) Three computed transition structures for the Michael addition of diethyl malonate and β-nitrostyrene with Δ*G* values related to **196** and (b) experimental KIE and computed (italics) KIE for C–C bond forming step as the rate-determining step.

for halide abstraction and substitution reactions [2, 9, 10]. In 2002, Wenzel and Jacobsen used a Schiff base catalyst in asymmetric Mannich reactions for the synthesis of β-aryl-β-amino acids and proposed an activation of the utilized *N*-Boc aldimines through hydrogen bonding [368], similar to the proposed activation mode in Strecker reactions by Vachal and Jacobsen (*vide supra*) [351]. In 2004, based on the work of Wenzel and Jacobsen, Taylor and Jacobsen presented the cyclization of indole derivatives **200** because of an asymmetric acetyl Pictet–Spengler reaction and suggested a similar activation mode [338]. The authors screened various thiourea derivatives, such as Schiff base **182** (cf. Scheme 1.40). Utilizing acetic anhydride, Taylor and Jacobsen did not observe product formation, even at high temperatures (Pictet–Spengler conditions). Switching to acetyl chloride as the acetylation reagent, the authors obtained the product in 65% and 59% *ee* catalyzed with 10 mol% **182**. After structure optimization of the catalyst, **199** was described as the most active one, bearing 2-methyl-5-phenylpyrrole moiety instead of the salicylaldehyde unit in **182** (70% yield; 93% *ee*). The authors described activation of the acyl-iminium ion by the thiourea's N–H protons and obtained Pictet–Spengler products **201** in yields ranging from 65% to 81% and *ee*-values of 86–95%, utilizing 5 or 10 mol% catalyst loading, whereby the imine substrate was generated *in situ* by condensation of the tryptamine derivatives with the corresponding aldehyde (Scheme 1.46). Furthermore, the products could be easily converted to tetrahydro-β-carbolines that are core structure elements in natural compounds [369, 370].

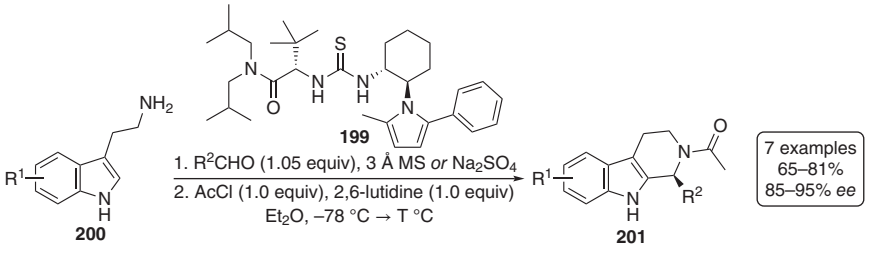


**Scheme 1.46** Asymmetric acetyl Pictet–Spengler reaction catalyzed with 5 or 10 mol% **199**.

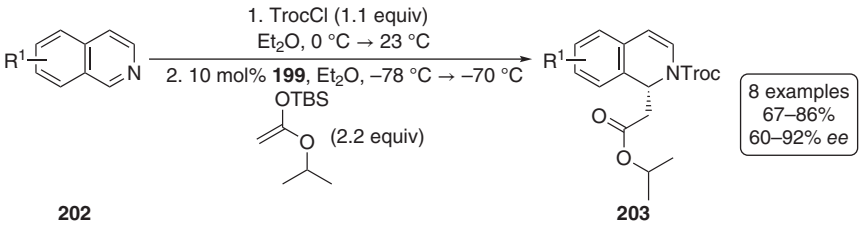


**Scheme 1.47** Enantioselective acyl-Mannich reactions utilizing various substituted isoquinolines catalyzed with **199**.

In 2005, the same group utilized **199** in asymmetric acyl-Mannich reactions of isoquinolines **202** and obtained substituted dihydroisoquinolines **203** in yields ranging from 67% to 86% and *ee*-values of 60–92%, utilizing 10 mol% catalyst loading (Scheme 1.47) [371]. Additionally, Jacobsen's group observed in the acyl-Mannich as well as in the acyl Pictet–Spengler reactions a pronounced solvent effect, with diethyl ether providing the highest *ee*-values. The authors pointed out that the nature of the acyl-imine adduct is important in the reaction and deemed TrocCl the best acylation reagent, with *tert*-butyldimethylsilyl ketene acetal being the most reactive nucleophile. Bose, Spiegelman, and Manhas observed in the acylation of benzylimine with various acyl chlorides the formation of a covalent chloroamide in non-polar solvents, such as carbon tetrachloride [372]. Based on this work, and because of the strong leaving group effect of the acylation reagent and the high enantioinduction in non-polar solvents, such as diethyl ether, Jacobsen's group postulated the presence of the chloroamide structure, rather than the *N*-acylium chloride structure of the acyl-imine adduct [371].

In 2007, Jacobsen's group presented the enantioselective Pictet–Spengler-type cyclization of β-indolyl ethyl hydroxy lactams **205** utilizing TMSCl as a dehydrating agent to form *in situ* and irreversibly the corresponding chloride derivatives [373]. The hydroxy lactam substrates were synthesized either by imide reduction utilizing $NaBH_4$ or by imide alkylation with organolithium reagents. The authors obtained the cyclization products **206** in yields ranging from 51% to 94% and *ee*-values of 81–99%, utilizing pyrrole-based catalyst **204** (Scheme 1.48), which is the *N*-methylpentyl amide derivative of **199** (cf. Scheme 1.46) [373].

Jacobsen's group also investigated the mechanism using substituent-, counterion-, solvent-, and kinetic isotope effects and variable temperature $^1$H NMR studies and

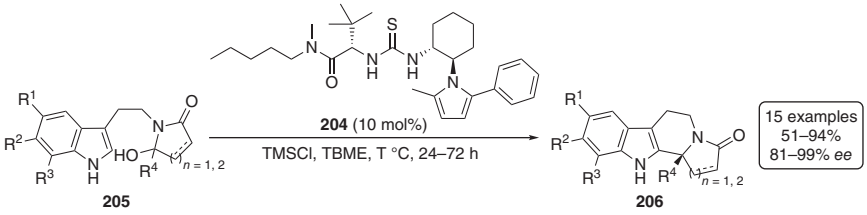


**Scheme 1.48** Asymmetric Pictet–Spengler-type cyclization of hydroxy lactams *via in situ* generation of iminium ions catalyzed with **204**.

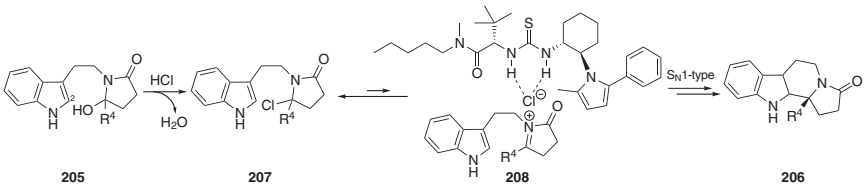


**Scheme 1.49** Proposed mechanism for the enantioselective Pictet–Spengler-type cyclization of β-indolyl ethyl hydroxy lactams **205** with thiourea **204**.

suggested that the reaction starts with the TMSCl-induced formation of a chlorolactam, comparable to the chloroamides in the acyl Mannich reaction (cf. Scheme 1.47). Subsequently, the product forms through either an $S_N2$-type mechanism or a stepwise $S_N1$ route involving coordination of the chloride to the thiourea. Multiple observations indicate the stepwise mechanism (Scheme 1.49):

(1) The reaction rate was much higher with substituents stabilizing positive charge in the α-position.
(2) There is a strong enantioselectivity dependence on the counteranion (Cl, 97% *ee*; Br, 68% *ee*; I <5% *ee*), supporting the stepwise mechanisms *via* anion binding.
(3) No KIE was observed in reactions utilizing indole with deuterated $C_2$, ruling out the possibility of a rate-limiting deprotonation/rearomatization step.
(4) NMR experiments of mixtures of the catalyst with tetrabutylammonium chloride (TBAC) resulted in a downfield shift of 0.56 ppm of thiourea N–H protons, while bromide as well as iodide counterions appear at lower downfield shifts. These results indicate the anion-binding mode [373].

This reaction is the second reported example for anion-binding catalysis utilizing hydrogen-bonding organocatalysts, after Kotke's and Schreiner's fundamental work (cf. Schemes 1.12 and 1.13) [176]. Nevertheless, this is the first mechanistic proposal that suggests that a hydrogen-bonding organocatalyst binds an anion in an enantioselective reaction [373], whereby it is generally excepted that also the acetyl Pictet–Spengler (Scheme 1.46) as well as the acyl-Mannich reactions (Scheme 1.47) are catalyzed by anion-binding interactions [9, 10]. A similar chloride-binding concept was applied in many other anion-binding catalyzed reactions [2, 9, 10], e.g., Jacobsen and coworkers utilized a similar activation mode in the biomimetic cyclization of hydroxy lactams [339], which is based on the polycyclization of *N*-acyliminium ions of Dijkink and Speckamp of the 1970s [374, 375]. The idea was to convert the hydroxy lactams *in situ* into the corresponding chlorolactams and to use a bifunctional catalyst that activates the chlorolactams by anion abstraction while stabilizing the cationic intermediates **211** [339]. The authors utilized HCl for the *in situ* formation of the chlorolactams and 4 Å molecular sieve for water removal. Using **209** as a model substrate and starting from thiourea **212** (10%, 9% *ee*), the authors performed catalyst optimization and introduced a conformationally rigid pyrrolidine substituent with an additional stereogenic center (Scheme 1.50).

Catalyst **213** afforded product **210** in a slightly higher yield and increased enantioinduction (12%, 25% *ee*). Changing the phenyl-substituent to 1- and 2-naphthyl substituents, increased catalyst reactivity and stereoselectivity were observed

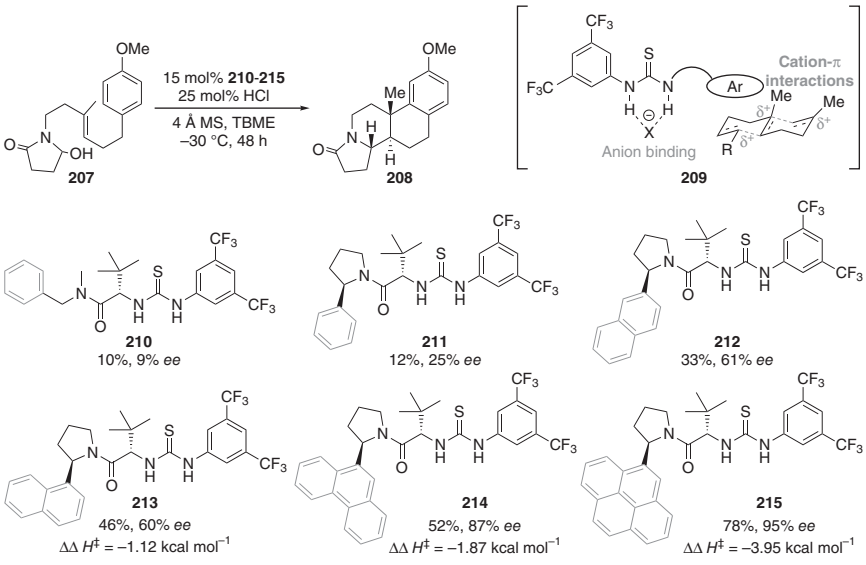


**Scheme 1.50** Catalyst optimization for hydroxy lactam polycyclization and stabilization of the cationic intermediate **211**. For catalysts **215—217**, different activation enthalpies are given.

(46%, 60% *ee*; 33%, 61% *ee*, respectively). The 9-phenanthryl-substituted derivative **216** furnished **210** with a slightly decreased yield (52%) but increased enantioselectivity (87% *ee*). In the last optimization step, Jacobsen's group introduced the 4-pyrenyl substituent and obtained **210** with a good yield (78%) and a high *ee*-value (95% *ee*). Notably, the authors observed with all catalysts depicted in Scheme 1.50 the formation of one single diastereomer of 210, whereas performing the reaction without thiourea catalyst only monocyclic products were obtained [339].

With the optimized catalyst in hand, Jacobsen's group synthesized tetracyclic products **219** in yields ranging from 51% to 77% and *ee*-values of 89–94% and a typical TOF value of 0.07 $h^{-1}$ (Scheme 1.51) [339]. The fact that the enantioinduction depends strongly on catalyst size, the authors noted that stabilizing cation–π interactions might play a key role in the intermediate as well as transition structure

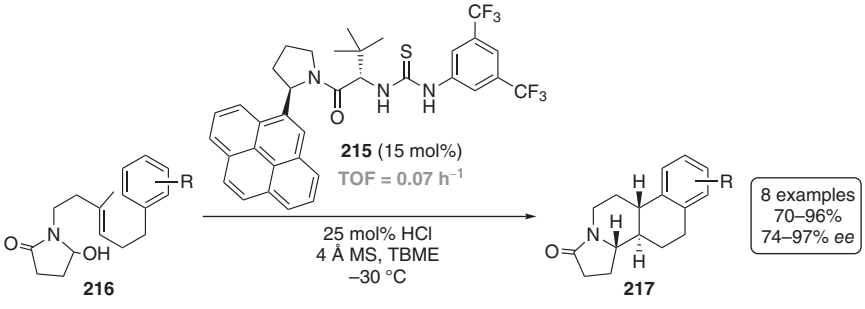


**Scheme 1.51** Polycyclization of hydroxy lactams *via in situ* generation of the cationic intermediate catalyzed with **217**.

stabilization. Because catalysts **215–217** displayed a linear correlation between ln(*e.r.*) and reciprocal temperature over a 70 °C range, an Eyring analysis of the enantioselectivity revealed that the enantioselectivity was enthalpically controlled. Furthermore, the differential enthalpy increased obviously as the catalyst arene increased in size and was only attenuated slightly by increased differential entropy terms. These data support the importance of cation–π stabilization as the essential component in the mechanism [339].

Another example utilizing the *in situ* generation of an electrophile through chloride abstraction is the enantioselective addition to oxocarbenium ions generated from 1-chloroisochromans **220** [242]. Reisman, Doyle, and Jacobsen utilized 10 mol% of thiourea **223** and various silyl ketene acetals **221** as nucleophiles and obtained **222** in yields ranging from 70% to 96%, *ee*-values of 74–95%, and TOF = 1.45 $h^{-1}$ (Scheme 1.52). The corresponding 1-chloroisochromans were prepared in a one-pot, two-stage procedure from the corresponding methyl acetals [242].

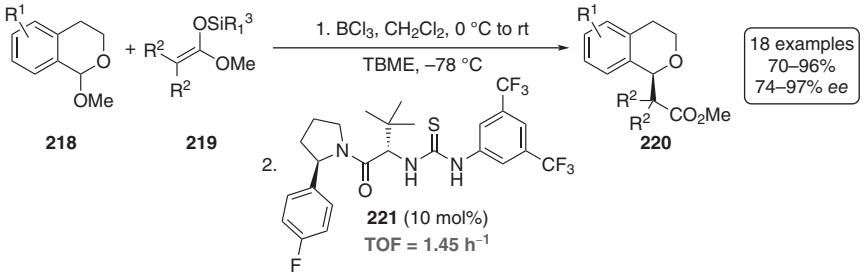


**Scheme 1.52** Addition from various silyl ketene acetals to *in situ* generated oxocarbenium ions catalyzed with **223**.

In 2016, Jacobsen's group investigated the activation mode of the **223**-catalyzed chloride abstraction reaction [241, 376–378]. In "same-excess" experiments in the alkylation of 1-chloroisochroman, the authors did not observe catalyst deactivation through decomposition pathways or by product inhibition [376]. Additionally, the catalyst's reaction rate at high loading (>5 mol%) was found to be first order, while non-linear behavior was observed at low catalyst loading, and a positive non-linear relationship between product *ee* and catalyst *ee* was identified. The authors observed three head-to-tail catalyst dimers in 2D NOESY NMR studies, where each thiourea moiety forms hydrogen bonds to the amide oxygen, and that this agglomeration leads to an "off-cycle aggregation" event [376]. Furthermore, the authors obtained single crystals of dimeric catalyst complexes of $[(Z\text{-}\mathbf{223})_2\cdot\mathbf{Cl}]_2^-$ by addition of tetramethylammonium chloride. The X-ray single-crystal analysis shows the formation of a 4H–anion-binding mode with the four N–H protons of the thiourea moiety, and the authors suggested a cooperative and structurally similar chloride abstraction through two catalyst molecules *via* 4H–anion binding (Scheme 1.53) [376].

Jacobsen's group described pairwise catalyst combinations leading to four transition structures (*ZZ*–TS, *EE*–TS, *ZE*–TS, and *EZ*–TS) that apparently all make contributions to the overall reaction rate and enantioselectivity [241]. To suppress the (*Z*)-(*E*)-amide isomerization, the authors performed computational

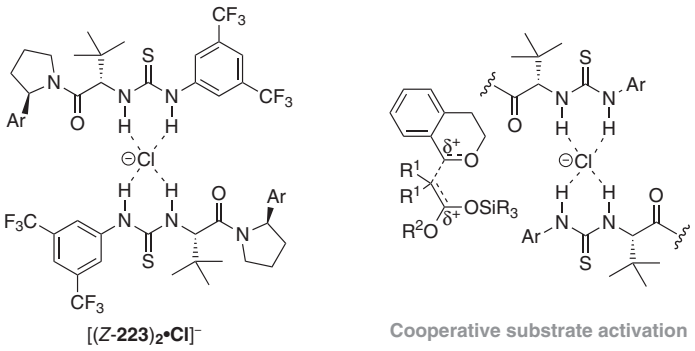


**Scheme 1.53** Structures of the bis-thiourea coordinated chloride found in X-ray single-crystal analysis and the cooperative activation *via* the 4H–anion-binding mode.

analyses at the B3LYP/6-31G+(d,p)//B3LYP/6-31G(d) level (at 0 K, not taking zero-point vibrational energy corrections or dispersion interactions into account) of the relative energies of thiourea rotamers bearing a variety of substituents on the pyrrolidine moiety and identified the 2-aryl-2-methylpyrrolidine-derived thiourea **224** as a promising candidate. Jacobsen *et al.* identified in $^{1}$H, $^{13}$C, and 2D NOESY NMR experiments only the (*Z*)-amide rotamer and showed the improved activity compared to **224** with **223** in the oxocarbenium alkylation, where both yield and enantioselectivity increased (Scheme 1.54) [241]. Based on these results – the 4H–anion-binding mode and the benefit of the conformationally rigid 2-aryl-2-methyl-pyrrolidine moiety – Jacobsen's group synthesized bis-thiourea **225** that showed strict first-order behavior, high rate acceleration compared to **223**, and also a linear relationship between product *ee* and catalyst *ee* [378]. These results provided strong clues for a monocatalyst activation process of **225**, and much higher activity was shown in the formation of **226**, utilizing 0.1 mol% **225** (at 100 times lower catalyst loading, cf. Scheme 1.52), eight times shorter reaction time, and five times higher concentration (Scheme 1.54) [378].

In 2017, Jacobsen's group published the stereospecific β-glycosylation of various sugars catalyzed with thiourea derivatives [379]. The idea was to mimic the glycosyltransferase-catalyzed glycosylation [380]. As depicted in Scheme 1.55, the *cis*-1,2-*O*-glycosylation of α-mannosyl chloride **229** was utilized as a model reaction because the β-glycosidic linkage is strongly disfavored both sterically and electronically [381].

The glycosylation utilizing benzyl alcohol in the absence of any catalyst furnished the α-product predominantly (84 : 16 α:β) with very low yield (0.1%), whereas with 5 mol% **223** slightly higher reactivity, but no selectivity was observed (1%, 52 : 48 α:β). Nevertheless, this result showed that the thiourea catalyst could invert the selectivity, and bis-thiourea **231** leads to a very moderate yield and β-selectivity (15%, 20 : 80 α:β). To improve both the reactivity and selectivity, Jacobsen's group synthesized macrocyclic derivate **232** that forms **230** in good yield and β-selectivity (68%, 12 : 82 α:β). The introduction of a 2,3-dihydroindole instead of the pyrrolidine moiety

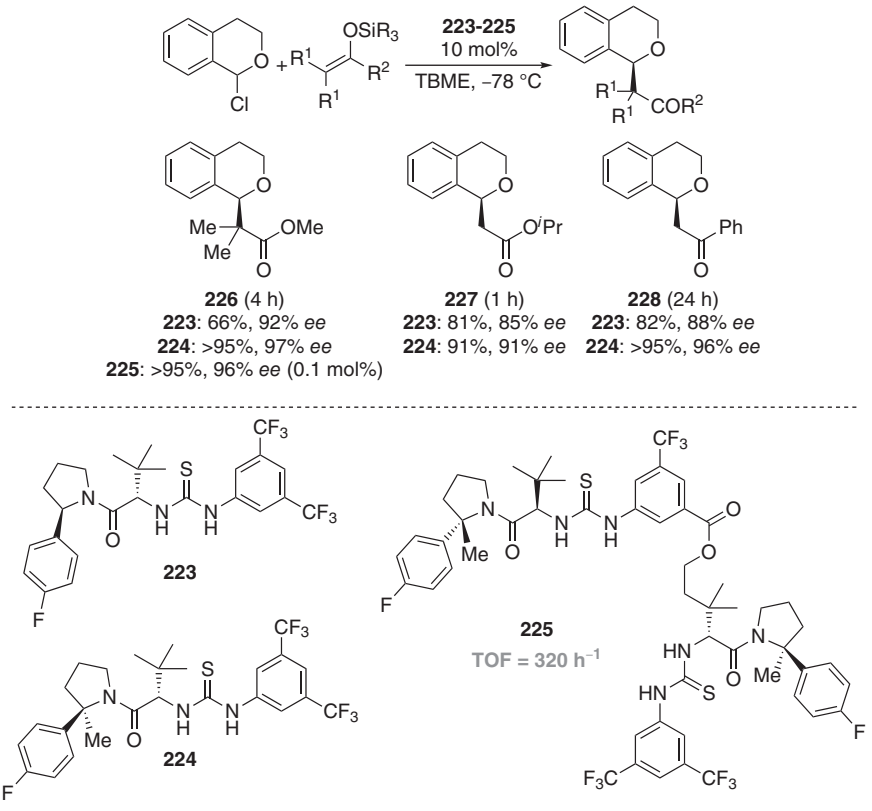


**Scheme 1.54** Comparison of the enantioselective oxocarbenium alkylations utilizing thiourea **223**, conformational rigid **224**, and improved bis-thiourea **225**.

resulted in catalyst **233** that furnished the product in high yield as well as high β-selectivity (88%, 8 : 92 α:β) [379].

With the optimized catalysts in hand, the authors synthesized various disaccharides utilizing α-glycosyl chlorides **234** and obtained **235**–**240** in yields ranging from 64% to 88% and as predominantly β-linked products (Scheme 1.56) [379]. The thiourea activation of the leaving group (chloride) promotes both the $S_N1$ and $S_N2$ pathways, but nucleophile activation would exclusively support the $S_N2$ pathway. Overall, Jacobsen's group suggested an $S_N2$ mechanism based on the following observations:

(1) The products were obtained with a high degree of inversion.
(2) The reaction was insensitive to relative catalyst–substrate as well as nucleophile–electrophile stereochemical relationships.
(3) No limitations concerning the substrate scope could be observed.

The authors assumed an activation of the nucleophile by the catalyst's amide oxygen that acts as a Lewis base and found in DFT studies (M06-2X/6-31G(d) with PCM:benzene solvent inclusion, no temperature given) on the concerted

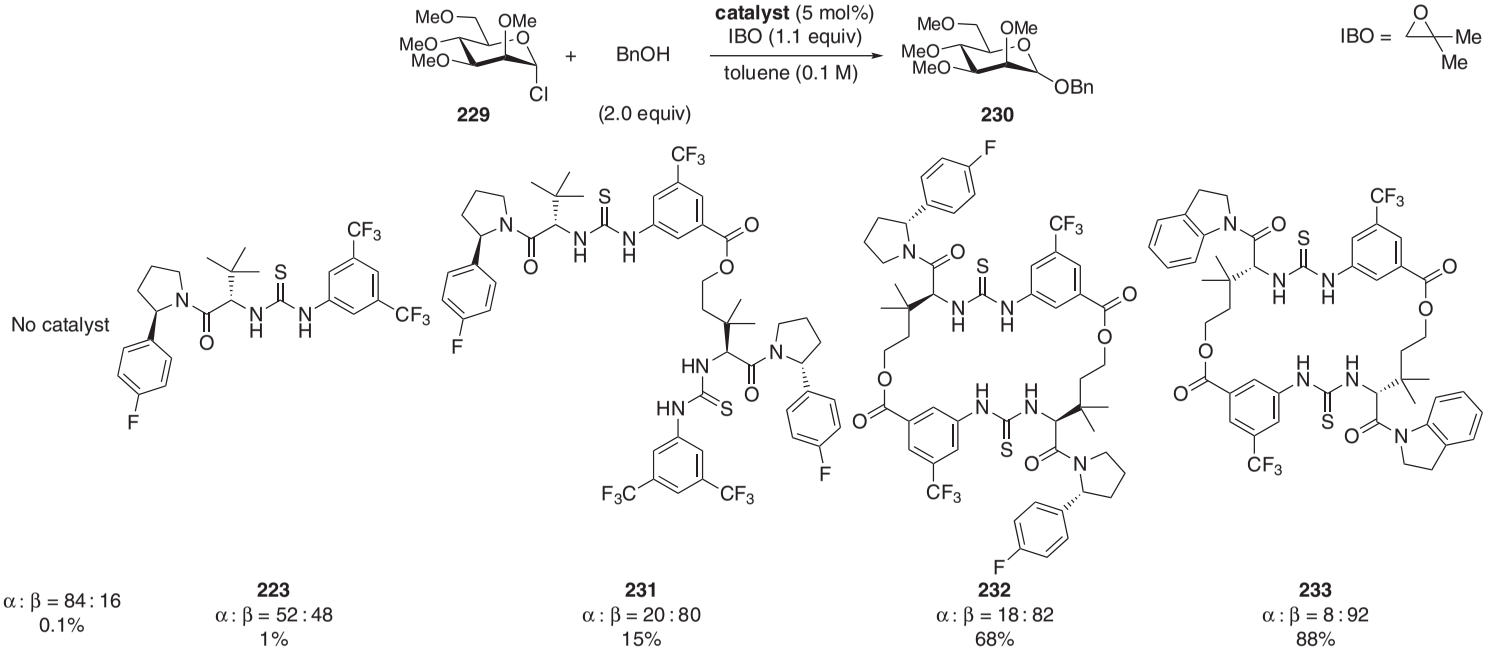


**Scheme 1.55** Evolution of thiourea catalysts for the *cis*-1,2-*O*-glycosylation of mannosyl chloride utilizing benzyl alcohol as nucleophile and IBO as the HCl trapping agent.

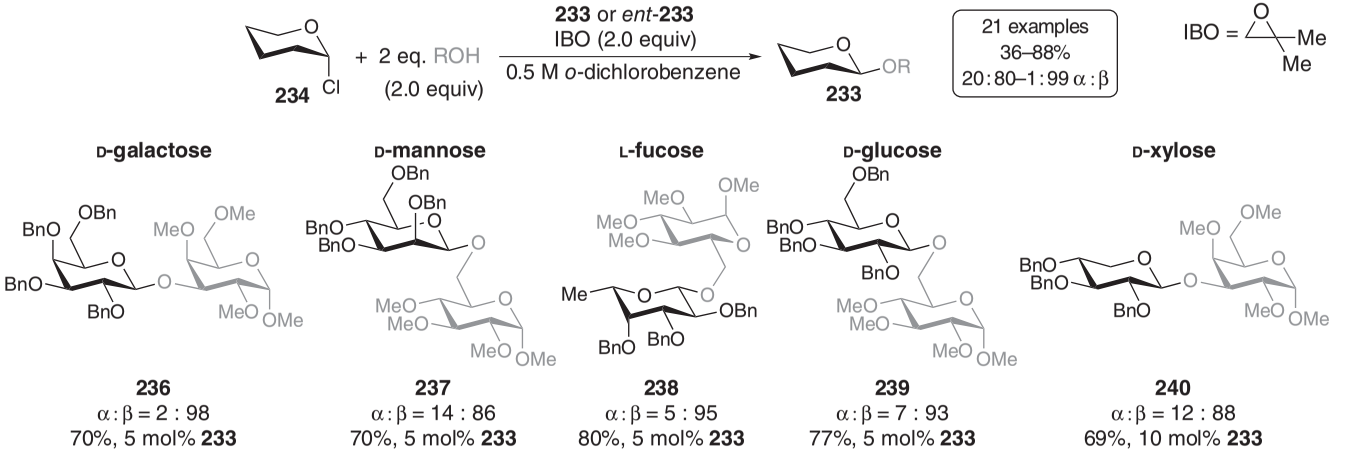


**Scheme 1.56** Typical glycosylation products with high β-selectivity utilizing macrocyclic bis-thioureas **233** or *ent*-**233**.

glycosylation of glucosyl chloride by methanol a loose and asynchronous transition structure with hydrogen-bonding interactions between the methanol O–H and the amide oxygen that supported the $S_N2$ mechanism by both leaving group as well as nucleophile activation [379].

In 2014, on expanding from achiral triazole-based anion-binding catalyst **114** (Scheme 1.25) [229, 230], Mancheño's group introduced helical chiral derivatives with a chiral 1,2-diaminocyclohexane backbone [231]. The idea was to synthesize a flexible catalyst structure that in the "non-active mode" will be present in an equilibrium between linear and helical conformations, and that in the complexation mode to a chloride anion, the helical system is the dominant species. The authors synthesized a series of helical triazole-based anion-binding catalysts **243–247** and tested them in the Reissert-type reaction of quinolone **241** utilizing silyl ketene acetals as nucleophiles. Using bis-triazole-based catalyst **243** that cannot adopt helical chirality upon chloride binding, the observed enantioinduction was low (18% *ee*). Going on to tetra-triazole-based catalysts such as **243–247**, Mancheño's group obtained product **242** with increased *ee*-values (62–92% *ee*) and observed that the substitution pattern of the central phenyl ring was important with the 2-(methoxy-propan-2-yl)acetylene substituent as the most active one. The difference between catalysts **246** and **247**, where the connection of the phenyl groups by the triazole units was slightly changed, was marginal (90% *ee* and 92% *ee*, respectively) [231]. To validate the anion-binding mode of **247**, the authors performed NMR titration experiments with Troc-quinolinium chloride and observed that the eight hydrogens, which are highlighted in Scheme 1.57, form hydrogen bonds to the chloride [231]. Additionally, circular dichroism (CD) titration of **247** with TBAC showed conformational changes in the folding behavior of the flexible oligomer. Increased absorption bands as 250 and 265–280 nm in the positive as well as negative regions of the UV spectrum indicated catalysts' chloride binding and the formation of the helical chiral form. Furthermore, the authors synthesized a series of Reissert-type products utilizing 5 mol% of **247** and obtained products in yields ranging from 54% to 96% and *ee*-values of 44–96% [231].

### 1.2.4 Anion Binding in Cooperative Catalysis

Besides the high ability to coordinate with chloride (cf. Section 1.2.3), (thio)ureas are well-known receptors for Y-shaped anions, such as carboxylates [135, 138, 382, 383]. The topology of these coplanar anions allows a bidentate hydrogen-bonding mode with an N–H···O angle of approximately 170–175° that leads to anion stabilization [384, 385]. Dual thiourea/carboxylic acid catalyst systems have been utilized in many anion-binding mode-catalyzed reactions, e.g., the alcoholysis of styrene oxides [291], protio Pictet–Spengler reactions [169, 386, 387], [5+2] cycloadditions [388], and, in particular, kinetic resolution of primary amines [342, 343, 389–393], a topic that was reviewed by Seidel in 2014 [341]. The general concept of dual-catalyst kinetic resolution is based on the *in situ* formation of a chiral acylating reagent and consists of three components: a pyridinium species (most reactions use 4-dimethylaminopyridine (DMAP) [393] or its derivatives, e.g.,

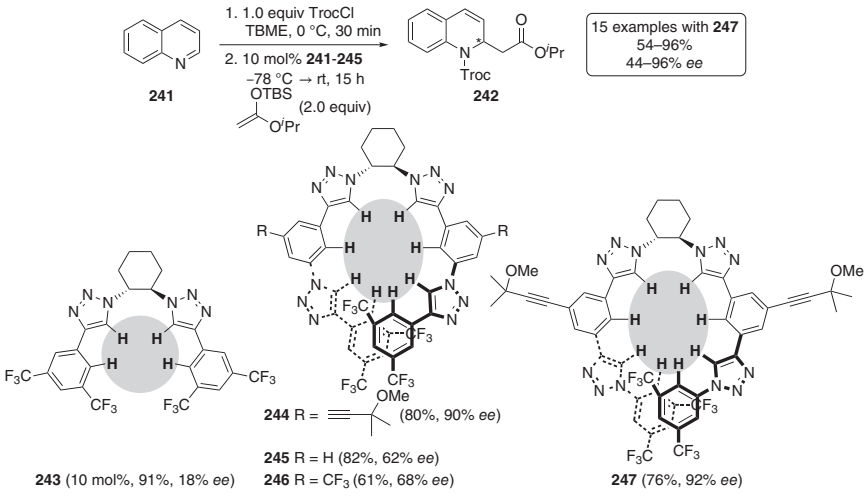


**Scheme 1.57** Optimization of helical chiral catalyst structure in Reissert-type reactions. Hydrogens coordinating the chloride are highlighted.

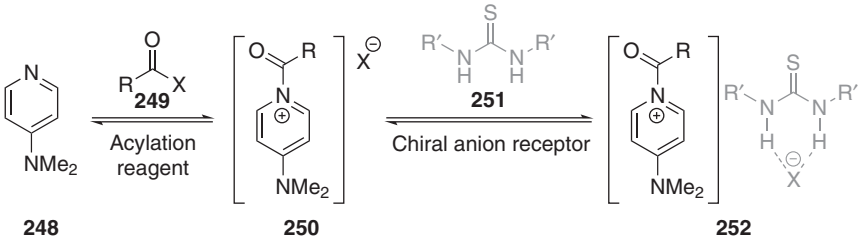


**Scheme 1.58** Anion-binding concept for formation of chiral supramolecular ion pairs that serve as chiral acyl transfer species.

4-(pyrrolidino)pyridine (PPY) [390]), an achiral acylating reagent, and a chiral anion-binding/hydrogen-bonding catalyst. Mixtures of DMAP **248** and acylating reagents **249** exist in equilibrium with the corresponding achiral acylpyridinium salt **250** [394]. Chiral catalyst **251** binds the anion, leading to supramolecular chiral ion pair formation that affects the equilibrium between DMAP and its acylpyridinium salt because the supramolecular ion **252** is generally more soluble in organic solvents. Consequently, the substrates should rather react with the chiral supramolecular ion pair than with the acylpyridinium salt (Scheme 1.58).

Because the nature of the chiral supramolecular ion complex was at that time unknown, Seidel, Schreiner, and coworkers investigated the mechanism of the dual-catalysis anion-binding approach in the kinetic resolution of amines utilizing both experimental and computational approaches [393]. Based on the original study by Seidel's group in 2009 [342], Seidel, Schreiner, and coworkers utilized 1-phenylethylamine *rac*-**253** as a model substrate, DMAP as pyridinium species, and tested a series of chiral catalysts. Starting catalyst evolution with the "original" bis-thiourea **256** (s-factor = 8.5), amide–thiourea catalyst **257** (s-factor = 13.0),

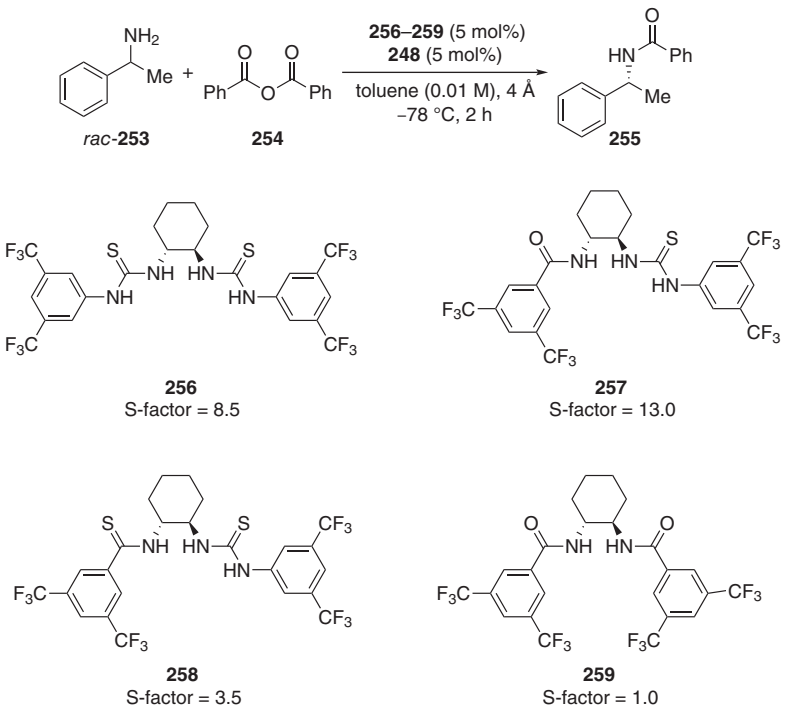


**Scheme 1.59** Catalyst evolution for kinetic resolution of 1-phenylethanamine utilizing various catalysts with DMAP as cocatalyst.

which was also utilized in kinetic resolution of primary amines [341], was found to be the most selective catalyst. In the catalyst evolution study, Seidel, Schreiner, and coworkers found that the thiourea as well as the amide moieties are crucial for high selectivity because the corresponding thioamide–thiourea **258** (s-factor = 3.5) and diamide **259** (s-factor = 1.0) were much less selective (Scheme 1.59) [393]. Using various acylating reagents, the authors obtained the highest selectivities with benzoic anhydride but could not identify a trend regarding the electronic nature utilizing substituted benzoic anhydride derivatives ($(4\text{-}CF_3\text{–}PhCO)_2O$ s-factor = 7.5; $(4\text{-Me–PhCO})_2O$ s-factor = 12.8; $(4\text{-MeO–PhCO})_2O$ s-factor = 4.8) [393]. Because the catalyst–substrate ion pairing is obviously crucial for the selectivity, toluene (s-factor = 13.0) was found as the solvent that furnished the highest *s*-value, as it favors (contact) ion pairs, whereas more polar solvents, such as ethyl acetate (s-factor = 1.5), resulted in solvent-shared or solvent-separated ion pairs (cf. Section 1.2.1) [326, 327].

Because deprotonation of the thiourea moiety would lead to an alternative ion pair, the authors performed deprotonation studies and identified hydrogen-bonding interactions between the catalyst's N–Hs and various amines, such as DMAP, Hünig's base, and 1-phenylethylamine in $^1$H NMR experiments, but could not observe a deprotonated catalyst species, which should be easily identifiable by shifts in the $^{13}$C NMR spectrum [143, 189]. These findings confirm the structure

of supramolecular ion pair **252**. Only when the stronger base BEMP was utilized, the deprotonated catalyst could be identified in the $^{1}H$ and $^{13}C$ NMR spectra. Using DFT-based computations ($\Delta H_0$, $D_0$, and $\Delta G$ values at M06/6-31G(d,p) including PCM solvent corrections for toluene at various temperatures), Seidel, Schreiner, and coworkers obtained for the ion pair of DMAP and benzoic anhydride substantial and negative dissociation energy ($D_0 = -6.8\,\text{kcal mol}^{-1}$; $D_{298} = -22.2\,\text{kcal mol}^{-1}$), which is consistent with the absence of NOE signals in NMR experiments; however, this could also be due to long proton–proton distances and fast exchange. Nevertheless, DOSY NMR spectroscopy equally did not reveal evidence of ion pair formation. Utilizing bis-thiourea **256**, the authors obtained a positive dissociation energy for ternary complex **252** (Scheme 1.58) in the gas-phase ($D_{195} = +10.4\,\text{kcal mol}^{-1}$) as well as in solution (toluene, $D_{195} = +3.6\,\text{kcal mol}^{-1}$), with **256** displaying (*Z,Z*)-oriented N–H protons. Additionally, Seidel, Schreiner, and coworkers identified that the benzoyl group is fixed in the ternary complex through π–π stacking with one of the thiourea aryl rings. Adding the (*R*)-configured amine, the lowest lying quaternary complex was found to coordinate the benzoate through double hydrogen bonding by one thiourea moiety, whereas the second thiourea unit coordinates the first thiourea moiety also through hydrogen bonding. Simultaneously, benzoate binds to the ortho and meta protons of the pyridinium cation. In this quaternary complex, the authors found threefold π–π stacking of one thiourea aryl, DMAP's pyridine, and the 1-phenylethylamine ring. Accordingly, quaternary complex formation was observed at −78 °C ($D_{195} = +19.0\,\text{kcal mol}^{-1}$; $D_{298} = +3.1\,\text{kcal mol}^{-1}$), whereas with the (*S*)-configured amine, the quaternary complex was less favorable ($D_{298} = +0.7\,\text{kcal mol}^{-1}$). Utilizing amide–thiourea catalyst **257**, the authors also found a (*Z,Z*)-oriented thiourea unit that binds the benzoate through double hydrogen bonding. Additionally, the acidified ortho-proton of the 3,5-bis(trifluoromethyl)phenyl moiety forms a hydrogen bond to one of the benzoate oxygens [190], and, similar to **256**, the amide binds *via* an N–H···S interaction to the thiourea. Benzoate forms hydrogen-bonds to DMAP's ortho proton, which itself is fixed by the two aryl groups of the catalyst, leading to a well-defined binding pocket. The dissociation energy is negative at 298 °C ($-0.5\,\text{kcal mol}^{-1}$) but positive at −78 °C ($+12.6\,\text{kcal mol}^{-1}$; $+5.2\,\text{kcal mol}^{-1}$ in toluene). These mechanistic studies using a combination of experimental as well as computational studies emphasize the high relevance of NCIs in anion-binding catalysis for the formation of a well-defined binding pocket that can furnish reactions with high stereoinduction [393].

### 1.2.5 Anion-Binding in Lewis Acid Enhancement Catalysis

In 2011, Schreiner's group utilized silicon–thiourea Lewis acid **260** in the House–Meinwald rearrangement of tri-substituted epoxides **261** and obtained the corresponding quaternary aldehydes **262** in yields of 43–88% (Scheme 1.60) [189]. Catalyst **260** forms by deprotonation of **46** and addition of $SiCl_4$ as evident from IR, NMR, and MS experiments. In blind experiments utilizing either **46** or $SiCl_4$, the authors did not observe product formation, which confirmed

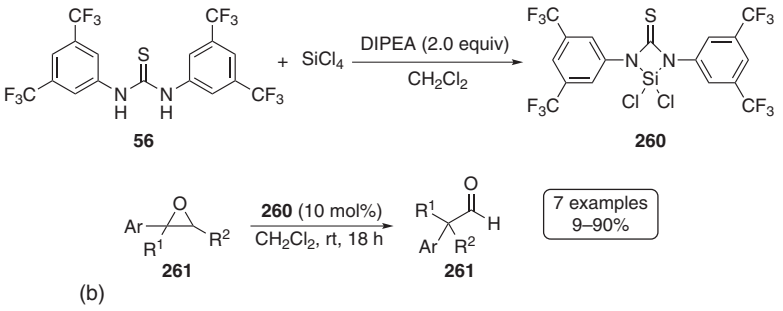


**Scheme 1.60** (a) Synthesis of silicon-thiourea Lewis acid through deprotonation of **56** and (b) House–Meinwald rearrangement utilizing tri-substituted epoxides.

the increased Lewis acidity of **260**. When utilizing enantioenriched epoxides, synthesized by Shi epoxidation [395], the authors observed increased enantiopurity for the starting material as well as the product. They performed a negative control experiment spiking the reaction mixture with enantioenriched product. However, a corresponding autocatalytic process could be excluded as no chirality enhancement for the product was observed.

Schreiner and coworkers proposed that an epoxide coordinates the silicon first and forms the active catalyst species. Binding by another epoxide would consequently lead to diastereomeric transition structures and to diastereomeric matched and mismatched combinations. Therefore, the reaction was described as "*similar to a kinetic resolution of non-racemic starting materials*" [396]. This reaction utilized a thiourea-based complex that increased the silicon's Lewis acidity by covalent bond formation and not through anion binding. Nevertheless, this was a proof-of-concept study for Lewis acid enhancement utilizing (thio)ureas.

In 2017, Jacobsen's group took up this concept in the activation of triflates for the generation of oxocarbenium ions [344]. Using **263** as a model substrate in Mukaiyama aldol reactions, the authors screened various (thio)ureas and squaramides and observed that only squaramides catalyzed the aldol reaction, which was explained by squaramides' dual functionality [197–199]. Jacobsen's group employed squaramides with various dispersion energy donors and found 1-pyrenyl-substituted derivate **266** as the most active one (100% conversion, 88% *ee*, Scheme 1.61); it displays a structure similar to that of thiourea **217** (cf. Scheme 1.50). The importance of catalysts hydrogen-bonding donor motif was validated through the *N,N′*-dimethylated analog of **266** that promoted the aldol reaction only little and nearly without selectivity (43% conversion, 2% *ee*) [344].

Subsequently, Jacobsen's group utilized the **266**-silyl-triflate system in [4+3] cycloadditions of oxyallyl cations and furan derivatives **268** and obtained bicyclic **269** in yields of 55–98% and 66–96% *ee* as single diastereomers (Scheme 1.62) [344]. The authors performed kinetic analysis and found zero-order kinetics for furan derivatives **268**, first-order kinetics for the oxyallyl cation precursor **267** as well as squaramide catalyst **266**, and saturation kinetics for trialkyl silyl triflate (TESOTf). The kinetic data are consistent with a pre-equilibrium between **266** and TESOTf, and rate-limiting oxyallyl cation formation. To prove the formation of a

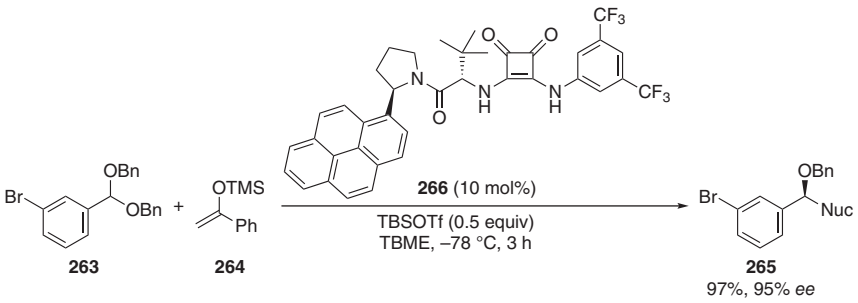


**Scheme 1.61** Representative example of enantioselective aldol reaction utilizing TBSOTf as Lewis acid and catalyst **266**.

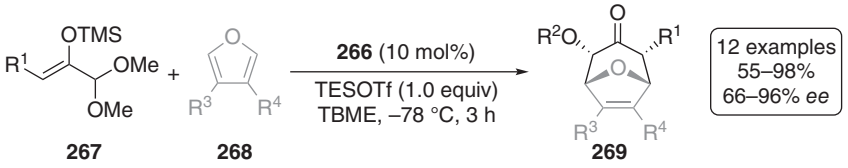


**Scheme 1.62** Enantioselective [4+3] cycloaddition catalyzed with **266** and TESOTf.

pre-equilibrium, the authors preformed $^1$H NMR experiments with $NBu_4OTf$ and TESOTf and observed stable complexes with both triflate species. However, TESOTf was found to bind 4000 times as strongly as $NBu_4OTf$ and forms simultaneous hydrogen bonds to the squaramides' N–Hs. While monitoring TESOTf addition to the squaramide catalyst utilizing IR spectroscopy, Jacobsen's group observed the disappearance of the absorbance attributed to the squaramide carbonyl groups. The authors proposed that complexation of **266** and trialkyl silyl triflates ($R_3SiOTf$) is more Lewis acid than ($R_3SiOTf$) alone because of the stabilization of the triflate anion through hydrogen-bonding interactions [344].

The authors suggested a catalytic cycle that starts with the resting state formation of the catalytically active enhanced Lewis acid **270** [344]. After the rate-determining ionization and generation of the oxyallyl cation, ion pair **271** forms. In a stepwise and enantiodetermining cycloaddition, the desired product forms and free enhanced Lewis acid **270** ensues (Scheme 1.63). Furthermore, the authors performed DFT studies (at the uncorrected M06-2X/6-31+G(d,p)//B3LYP/6-31G(d) level of theory) and identified transition structures leading to the formation of the major and minor products. Jacobsen's group described that the furan position near the catalyst's aromatic substituent leads to a stabilization of the major enantiomer trough NCIs, whereas the transition structure for the minor enantiomer lacks this stabilization [344].

### 1.2.6 Anion-Binding in Phase Transfer Catalysis

Fluorine incorporation in organic molecules leads to modified properties, such as lowering the p$K_a$ of the neighboring groups and changing molecules' dipole moments. In particular, sp$^3$ C–F bonds have a large influence on metabolic

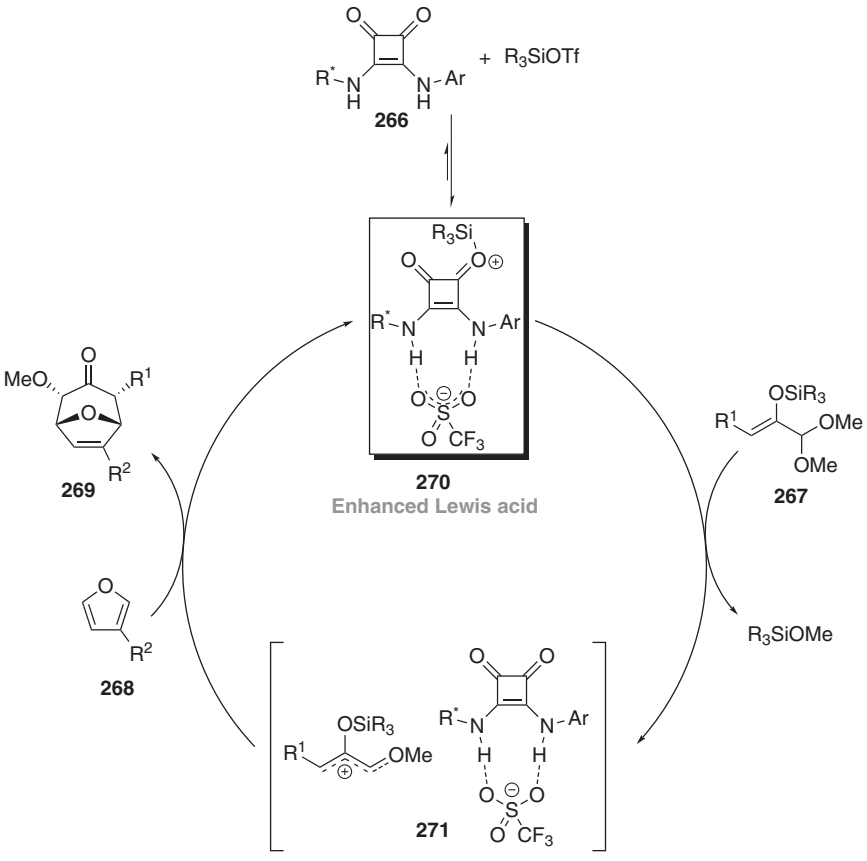


**Scheme 1.63** Pre-equilibrium leading to the formation of the enhanced Lewis acid 268 and the proposed catalytic cycle for the enantioselective [4+3] cycloaddition.

stability, lipophilicity, and bioavailability – characteristics that are highly important in pharmaceutical science [397–402]. Gouverneur's group utilized urea-based phase transfer catalysts (PTC) [403–405] for the asymmetric nucleophilic fluorine incorporation [346–348] and utilized the well-known potent ability of ureas' fluoride recognition [384, 406–408]. Generally, fluorination is dominated by methods utilizing electrophilic fluorine species [409, 410] such as selectfluor [411]. Additionally, asymmetric PTC using organic electrophilic fluorine species are known [412, 413], whereas the anion-binding-mediated fluorination approach of Gouverneur's group based on cheap alkali-metal fluorides, such as cesium fluoride [346, 347] or potassium fluoride [348], mimic the nucleophilic enzymatic fluorination of *S*-adenosyl-L-methionine [414–416]. In 2016, Gouverneur and coworkers obtained single crystals by refluxing *N,N′*-bis(4-chloro)phenylurea and tetrabutylammonium fluoride (TBAF) in *n*-hexane. An X-ray crystal structure analysis of this complex revealed two different complexes with both urea moieties forming hydrogen bonds to the fluoride. The main difference of the two complexes is the twisted geometries as expressed through the interplanar angles of 40.6° and 76.3°. Gouverneur and coworkers synthesized tridentate and tetradentate catalysts

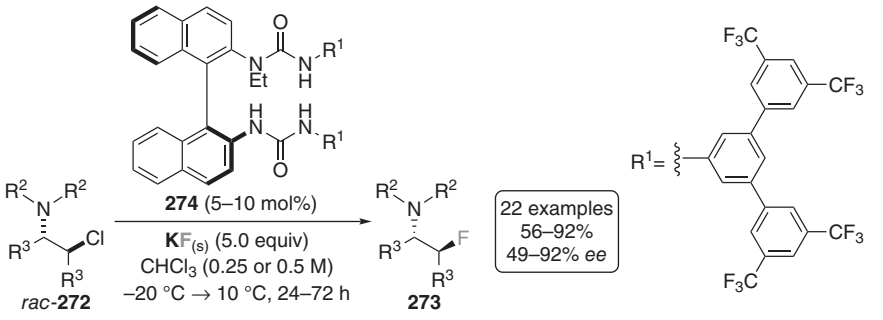


**Scheme 1.64** Generation of β-fluoroamines obtained by asymmetric PTC fluorination with bis-urea **274**.

with two urea units, the privileged 3,5-bis(trifluoromethyl)phenyl motif [190], and 1,1′-binaphthalene-2,2′-diamine (BINAM) as the chiral backbone. The authors observed higher enantioinduction using tridentate derivatives as monoalkyl incorporation into one urea resulted in a preferred *anti-syn* conformation and formation of a well-defined binding pocket [346]. In 2019 [347], the same group utilized anion-binding-mediated PTC for the enantioselective synthesis of β-fluoroamines **273** that are a highly relevant substance class in medicinal chemistry [417–420]. The idea was the *in situ* formation of a prochiral aziridinium species **276** (Scheme 1.65) that subsequently underwent ring opening by the fluoride. The authors optimized the catalyst and identified **274** as the most active catalyst incorporating additional 3,5-bis(trifluoromethyl)phenyl substituents (cf. Scheme 1.64). Utilizing 5–10 mol% of bis-urea **274**, β-fluoroamines were obtained in yields of 63–92% and 49–92% *ee* [348].

The authors utilized molecular dynamics (MD) simulations and DFT computations ($\Delta G$ values at ωB97X-D3/(ma)-def2-TZVPP/COSMO($CHCl_3$)//M06-2X/def2-SVP(TZVPPD)/CPCM($CHCl_3$)) to gain insights into the reaction mechanism [348]. The MD simulations reveal a preferred *anti-syn* conformation of the catalysts. Utilizing DFT computations, 15 optimized transition structures for ring-opening of bisaryl-based aziridinium species were found, with the lowest lying transition structure leading to the major product being favored by 1.6 kcal $mol^{-1}$. The most favorable transition structure for both major and minor enantiomer reveals that the aziridinium ion N-substituents are pointing away from the catalytic pocket into the solvent, thereby helping to rationalize the indifference to this substituent (Scheme 1.64). Furthermore, Gouverneur and coworkers found cation–π interactions between the naphthyl ring and the aziridinium Cα–H protons. The authors described stronger cation–π interactions for transition structure leading to the major enantiomer since the distance compared with the transition structure for the minor enantiomer was shorter (2.26 Å vs. 2.41 Å, respectively). Additionally, unfavorable geometric distortions due to steric crowding contribute with about 1.0 kcal $mol^{-1}$. The authors proposed a mechanism that starts with the formation of the soluble and chiral fluoride from inorganic and insoluble potassium fluoride. Additionally, Gouverneur and coworkers suggested an equilibrium of the racemic β-chloroamines **272** and the reactive aziridinium chloride ion pair **276**. Ion pairs **275** and **276** underwent

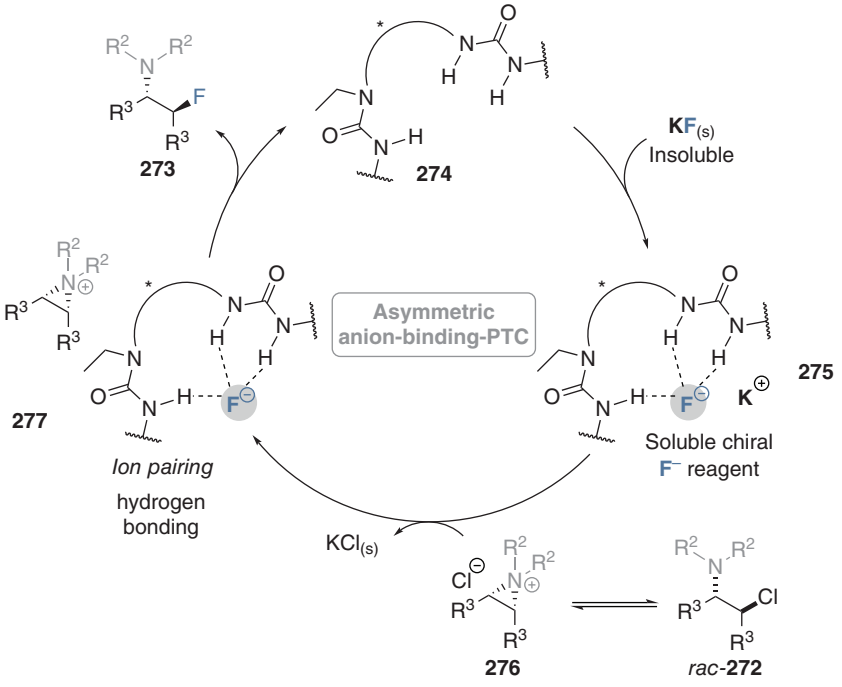


**Scheme 1.65** Proposed mechanism of the asymmetric hydrogen-bonding PTC to furnish enantioenriched β-fluoroamines, utilizing KF, racemic β-chloroamines, and bis-urea **274**.

an ion-change process leading to the formation of insoluble potassium chloride and supramolecular anion pair **277**. Nucleophilic addition to the aziridinium ion furnishes the desired product **273** and free catalyst **274** (Scheme 1.65) [348].

## 1.3 Summary and Outlook

This chapter reviews the long evolution in anion-binding chemistry starting with the first observations in the 1940s and 1950s and ending today with highly efficient organocatalysts that activate and direct reactions through anion binding. Starting with unselective (thio)ureas that show low TOF values ($<1\ h^{-1}$), in the last years, organic chemist designed highly active anion-binding organocatalysts for asymmetric induction with TOF values up to $4000\ h^{-1}$, thereby underlining the success story of anion-binding catalysts – after initial ignorance and skepticism in the early years. After the foundational work in the late 1990s and early 2000s, the growing interest in this research field has been exponential, as demonstrated by the milestone achievements and guidelines for (thio)urea catalyst design summarized and presented here. The evident success of these design principles for anion-binding catalysts also triggered the development of novel catalyst classes over the past few years, such as those binding through C–H hydrogen bonds and σ-holes and incorporating anion-binding motifs into switchable catalysts. One crucial design element in asymmetric

anion-binding catalysis is NCIs, including hydrogen-bonding, π–π as well as cation–π stacking, and dipole interactions. What is missing is the appreciation of London dispersion interactions (*via* dispersion energy donors, DEDs) as a design element. The inclusion of these interactions will finally complete all supposedly "weak" interactions that are at the heart of transition-state stabilization in a catalytic event.

The preferred use of non-polar solvents supports contact ion pair formation in intermediates and transition structures. In previous reviews, the authors divided organocatalysts in bound anion species, such as halide, enolate, and so on. In this chapter, we presented the five general activation modes in anion-binding catalysis utilizing selected representative examples, describing catalyst design principles, and presenting mechanistic proposals that go along with them:

(1) Recognition of the nucleophile in addition reactions and NCIs between the catalyst and the electrophile.
(2) Abstraction of the leaving group in $S_N1$-type reactions and formation of a chiral contact ion pair.
(3) Cooperative catalysis with an additional Brønsted acid forming a well-defined binding pocket to interact with the substrate.
(4) Lewis acid enhancement through activation by a Lewis base.
(5) Nucleophile delivery in phase transfer catalysis by nucleophile-binding and subsequent transfer into the organic medium.

Some important conceptual and practical points to be considered in future anion-binding-catalyzed reactions (and not only these) may include the following:

(1) To make catalyst reactivities and stereoselectivities more comparable, TOF values should be used and uncatalyzed reference reactions should always be reported.
(2) Typically, reactions are performed on a very small scale (0.1–0.2 mmol). To show the practicability of a new reaction, scale-up experiments (5–10 mmol) should be carried out to leave the "proof-of-concept" phase toward the challenging phase in which research should focus on broader, even large-scale applications.
(3) The product yields should be given and not just conversion of the starting materials because any side reaction also consumes the starting material. Furthermore – as we all know all too well – the work-up process is crucial for the isolation of a pure product. Only the yield determined for a sizeable amount of pure product matters when, for instance, it is to be used for (bio)medical applications.
(4) Novel applications in anion-binding catalysis should be investigated using experimental and theoretical studies to elucidate catalyst activation modes and principle mechanistic hypotheses.

## Acknowledgment

We gratefully acknowledge the financial support by the German Research Foundation (Deutsche Forschungsgemeinschaft) and the State of Hesse for the many years

of continuing support. We thank Raffael C. Wende and Bastian Bernhardt for valuable discussions.

## References


1 Schreiner, P.R. (2003). *Chem. Soc. Rev.* 32: 289–296.
2 Zhang, Z. and Schreiner, P.R. (2009). *Chem. Soc. Rev.* 38: 1187–1198.
3 Pihko, P.M. (2004). *Angew. Chem. Int. Ed.* 43: 2062–2064.
4 Takemoto, Y. (2005). *Org. Biomol. Chem.* 3: 4299–4306.
5 Connon, S.J. (2006). *Chem. Eur. J.* 12: 5418–5427.
6 Taylor, M.S. and Jacobsen, E.N. (2006). *Angew. Chem. Int. Ed.* 45: 1520–1543.
7 Akiyama, T., Itoh, J., and Fuchibe, K. (2006). *Adv. Synth. Chem.* 348: 999–1010.
8 Doyle, A.G. and Jacobsen, E.N. (2007). *Chem. Rev.* 107: 5713–5743.
9 Brak, K. and Jacobsen, E.N. (2013). *Angew. Chem. Int. Ed.* 52: 534–561.
10 Beckendorf, S., Asmus, S., and García Mancheño, O. (2012). *ChemCatChem* 4: 926–936.
11 Pihko, P.M. (2009). *Hydrogen Bonding in Organic Synthesis*. Weinheim: Wiley VCH.
12 Mahlau, M. and List, B. (2013). *Angew. Chem. Int. Ed.* 52: 518–533.
13 Auvil, T.J., Schafer, A.G., and Mattson, A.E. (2014). *Eur. J. Org. Chem.* 2014: 2633–2646.
14 Phipps, R.J., Hamilton, G.L., and Toste, F.D. (2012). *Nat. Chem.* 4: 603–614.
15 Schramm, V.L. (2006). *Chem. Rev.* 106: 3029–3030.
16 Watson, J.D. and Crick, F.H.C. (1953). *Nature* 171: 737–738.
17 Jeffrey, G.A. and Saenger, W. (1994). *The Role of Hydrogen Bonding in the Structure and Function of the Nucleic Acids*. Berlin: Springer.
18 Fonseca Guerra, C., Bickelhaupt, F.M., Snijders, J.G., and Baerends, E.J. (2000). *J. Am. Chem. Soc.* 122: 4117–4128.
19 Fersht, A. (1999). *Structure and Mechanism in Protein Science*. New York: Macmillan Education.
20 Gao, J., Ma, S., Major, D.T. *et al*. (2006). *Chem. Rev.* 106: 3188–3209.
21 Carey, P.R. (2006). *Chem. Rev.* 106: 3043–3054.
22 Boehr, D.D., Dyson, H.J., and Wright, P.E. (2006). *Chem. Rev.* 106: 3055–3079.
23 Bruice, T.C. (2006). *Chem. Rev.* 106: 3119–3139.
24 Antoniou, D., Basner, J., Núñez, S., and Schwartz, S.D. (2006). *Chem. Rev.* 106: 3170–3187.
25 Kirby, A.J. (1996). *Angew. Chem. Int. Ed.* 35: 706–724.
26 Kohen, A. and Klinman, J.P. (1998). *Acc. Chem. Res.* 31: 397–404.
27 Lindskog, S. (1997). *Pharmacol. Ther.* 74: 1–20.
28 Bruice, T.C. and Benkovic, S.J. (2000). *Biochemistry* 39: 6267–6274.
29 Williams, D.H., Stephens, E., O'Brien, D.P., and Zhou, M. (2004). *Angew. Chem. Int. Ed.* 43: 6596–6616.
30 Evans, M.J. and Cravatt, B.F. (2006). *Chem. Rev.* 106: 3279–3301.
31 Christianson, D.W. (2006). *Chem. Rev.* 106: 3412–3442.

**32** Pauling, L. (1960). *The Nature of the Chemical Bond*. Ithaca, NY: Cornell University Press.

**33** Pimentel, G.C. and McClellan, A.L. (1960). *The Hydrogen Bond*. San Francisco: W. H. Freemann.

**34** Jeffrey, G.A. and Jeffrey, G.A. (1997). *An Introduction to Hydrogen Bonding*. New York: Oxford University Press.

**35** Prins, L.J., Reinhoudt, D.N., and Timmerman, P. (2001). *Angew. Chem. Int. Ed.* 40: 2382–2426.

**36** Steiner, T. (2002). *Angew. Chem. Int. Ed.* 41: 48–76.

**37** Hunter, C.A. (2004). *Angew. Chem. Int. Ed.* 43: 5310–5324.

**38** Riordan, J., McElvany, K., and Borders, C. (1977). *Science* 195: 884–886.

**39** Riordan, J.F. (1979). *Mol. Cell. Biochem.* 26: 71–92.

**40** Riley, K.E. and Hobza, P. (2013). *Acc. Chem. Res.* 46: 927–936.

**41** Meyer, E.A., Castellano, R.K., and Diederich, F. (2003). *Angew. Chem. Int. Ed.* 42: 1210–1250.

**42** Dessent, C.E.H. and Müller-Dethlefs, K. (2000). *Chem. Rev.* 100: 3999–4022.

**43** Wear, M.A., Kan, D., Rabu, A., and Walkinshaw, M.D. (2007). *Angew. Chem. Int. Ed.* 46: 6453–6456.

**44** Warshel, A., Sharma, P.K., Kato, M. *et al*. (2006). *Chem. Rev.* 106: 3210–3235.

**45** Kraut, D.A., Sigala, P.A., Pybus, B. *et al*. (2006). *PLoS Biol.* 4: 201–519.

**46** Lau, E.Y., Newby, Z.E., and Bruice, T.C. (2001). *J. Am. Chem. Soc.* 123: 3350–3357.

**47** Hopmann, K.H. and Himo, F. (2006). *Chem. Eur. J.* 12: 6898–6909.

**48** Hopmann, K.H. and Himo, F. (2006). *J. Phys. Chem. B* 110: 21299–21310.

**49** de Vries, E.J. and Janssen, D.B. (2003). *Curr. Opin. Biochem.* 14: 414–420.

**50** Jormakka, M., Törnroth, S., Abramson, J. *et al*. (2002). *Acta Crystallogr. D* 58: 160–162.

**51** Hedstrom, L. (2002). *Chem. Rev.* 102: 4501–4524.

**52** Product inhibition and substrate inhibition are effects also known in enzyme catalysis that can reduce catalytic efficiency. Generally, catalytic systems (natural or artificial) based on covalent interactions are more sensitive towards inhibitions than non-covalent systems utilizing weak interactions:Garcia-Junceda, E. (2008). *Multi-Step Enzyme Catalysis*. Weinheim: Wiley-VCH.

**53** Vigny, M., Bon, S., Massoulié, J., and Leterrier, F. (1978). *Eur. J. Biochem.* 85: 317–323.

**54** Blackmond, D.G., Armstrong, A., Coombe, V., and Wells, A. (2007). *Angew. Chem. Int. Ed.* 46: 3798–3800.

**55** Sheldon, R.A. (2008). *Chem. Commun.* 44: 3352–3365.

**56** Murakami, Y., Kikuchi, J.-i., Hisaeda, Y., and Hayashida, O. (1996). *Chem. Rev.* 96: 721–758.

**57** Kirby, A.J. and Hollfelder, F. (2009). *From Enzyme Models to Model Enzymes*. Cambridge: Royal Society of Chemistry.

**58** Breslow, R. (2005). Artificial Enzymes. In: *Artificial Enzymes* (ed. R. Breslow), 1–35. Weinheim: Wiley-VCH.

**59** Breslow, R. (1982). *Science* 218: 532–537.

**60** Breslow, R. (1995). *Acc. Chem. Res.* 28: 146–153.
**61** Pascal, R. (2003). *Eur. J. Org. Chem.* 2003: 1813–1824.
**62** Egorova, K.S. and Ananikov, V.P. (2017). *Organometallics* 36: 4071–4090.
**63** Pauling, L. (1948). *Nature* 161: 707–709.
**64** Pauling, L. (1946). *Chem. Eng. News* 24: 1375–1377.
**65** Zhang, X. and Houk, K.N. (2005). *Acc. Chem. Res.* 38: 379–385.
**66** Jencks, W.P. (1980). *Acc. Chem. Res.* 13: 161–169.
**67** Jencks, W.P. (1976). *Acc. Chem. Res.* 9: 425–432.
**68** Warshel, A. (1981). *Biochemistry* 20: 3167–3177.
**69** Johnson, K.A. and Goody, R.S. (2011). *Biochemistry* 50: 8264–8269.
**70** Michaelis, L. and Menten, M. (1913). *Biochem. Z.* 49: 333–369.
**71** Bruice, T.C. (2002). *Acc. Chem. Res.* 35: 139–148.
**72** Fox, K.M. and Karplus, P.A. (1994). *Structure* 2: 1089–1105.
**73** Kawai, Y., Inaba, Y., and Tokitoh, N. (2001). *Tetrahedron: Asymmetry* 12: 309–318.
**74** Kawai, Y., Inaba, Y., Hayashi, M., and Tokitoh, N. (2001). *Tetrahedron Lett.* 42: 3367–3368.
**75** Meah, Y. and Massey, V. (2000). *Proc. Natl. Acad. Sci. U.S.A.* 97: 10733–10738.
**76** Bartlett, P.D. and Dauben, H.J. Jr., (1940). *J. Am. Chem. Soc.* 62: 1339–1344.
**77** Swain, C.G. (1948). *J. Am. Chem. Soc.* 70: 1119–1128.
**78** Lund, H. (1958). *Acta Chem. Scand.* 12: 298–302.
**79** Bufalini, J. and Stern, K.H. (1961). *J. Am. Chem. Soc.* 83: 4362–4366.
**80** Tsuboi, M. (1952). *Bull. Chem. Soc. Jpn.* 25: 60–66.
**81** Tsubomura, H. (1955). *J. Chem. Phys.* 23: 2130–2133.
**82** Allerhand, A. and v. R. Schleyer, P. (1963). *J. Am. Chem. Soc.* 85: 1233–1237.
**83** Simmons, H.E. and Park, C.H. (1968). *J. Am. Chem. Soc.* 90: 2428–2429.
**84** Park, C.H. and Simmons, H.E. (1968). *J. Am. Chem. Soc.* 90: 2429–2431.
**85** Park, C.H. and Simmons, H.E. (1968). *J. Am. Chem. Soc.* 90: 2431–2432.
**86** Bell, R.A., Christoph, G.G., Fronczek, F.R., and Marsh, R.E. (1975). *Science* 190: 151–152.
**87** Busschaert, N., Caltagirone, C., Van Rossom, W., and Gale, P.A. (2015). *Chem. Rev.* 115: 8038–8155.
**88** Molina, P., Zapata, F., and Caballero, A. (2017). *Chem. Rev.* 117: 9907–9972.
**89** He, Q., Vargas-Zúñiga, G.I., Kim, S.H. *et al*. (2019). *Chem. Rev.* 119: 9753–9835.
**90** Schmidtchen, F.P. and Berger, M. (1997). *Chem. Rev.* 97: 1609–1646.
**91** Kim, S.K. and Sessler, J.L. (2010). *Chem. Soc. Rev.* 39: 3784–3809.
**92** Park, I.-W., Yoo, J., Adhikari, S. *et al*. (2012). *Chem. Eur. J.* 18: 15073–15078.
**93** Gunnlaugsson, T., Glynn, M., Tocci, G.M. *et al*. (2006). *Coord. Chem. Rev.* 250: 3094–3117.
**94** Mutihac, L., Lee, J.H., Kim, J.S., and Vicens, J. (2011). *Chem. Soc. Rev.* 40: 2777–2796.
**95** Teresa Albelda, M., Frías, J.C., García-España, E., and Schneider, H.-J. (2012). *Chem. Soc. Rev.* 41: 3859–3877.
**96** Wichmann, K., Antonioli, B., Söhnel, T. *et al*. (2006). *Coord. Chem. Rev.* 250: 2987–3003.

**97** Moyer, B.A. (2013). *Ion Exchange and Solvent Extraction: Volume 21, Supramolecular Aspects of Solvent Extraction*. Boca Raton: CRC Press.

**98** Davis, A.P. (2006). *Coord. Chem. Rev.* 250: 2939–2951.

**99** Davis, A.P., Sheppard, D.N., and Smith, B.D. (2007). *Chem. Soc. Rev.* 36: 348–357.

**100** Matile, S., Vargas Jentzsch, A., Montenegro, J., and Fin, A. (2011). *Chem. Soc. Rev.* 40: 2453–2474.

**101** Davis, J.T., Okunola, O., and Quesada, R. (2010). *Chem. Soc. Rev.* 39: 3843–3862.

**102** Gale, P.A. (2011). *Acc. Chem. Res.* 44: 216–226.

**103** Behera, H. and Madhavan, N. (2017). *J. Am. Chem. Soc.* 139: 12919–12922.

**104** Busschaert, N. and Gale, P.A. (2013). *Angew. Chem. Int. Ed.* 52: 1374–1382.

**105** Gokel, G.W. and Barkey, N. (2009). *New J. Chem.* 33: 947–963.

**106** Lankshear, M.D. and Beer, P.D. (2006). *Coord. Chem. Rev.* 250: 3142–3160.

**107** Gimeno, N. and Vilar, R. (2006). *Coord. Chem. Rev.* 250: 3161–3189.

**108** Custelcean, R. (2014). *Chem. Soc. Rev.* 43: 1813–1824.

**109** Vilar, R. (2003). *Angew. Chem. Int. Ed.* 42: 1460–1477.

**110** Galbraith, E. and James, T.D. (2010). *Chem. Soc. Rev.* 39: 3831–3842.

**111** Nishiyabu, R., Kubo, Y., James, T.D., and Fossey, J.S. (2011). *Chem. Commun.* 47: 1106–1123.

**112** Hudnall, T.W., Chiu, C.-W., and Gabbaï, F.P. (2009). *Acc. Chem. Res.* 42: 388–397.

**113** Izzo, I., Licen, S., Maulucci, N. *et al.* (2008). *Chem. Commun.* 44: 2986–2988.

**114** Caballero, A., Zapata, F., White, N.G. *et al.* (2012). *Angew. Chem. Int. Ed.* 51: 1876–1880.

**115** Hine, J., Ahn, K., Gallucci, J.C., and Linden, S.M. (1984). *J. Am. Chem. Soc.* 106: 7980–7981.

**116** Hine, J., Linden, S.M., and Kanagasabapathy, V.M. (1985). *J. Am. Chem. Soc.* 107: 1082–1083.

**117** Hine, J., Linden, S.M., and Kanagasabapathy, V.M. (1985). *J. Org. Chem.* 50: 5096–5099.

**118** Errera, J. and Mollet, P. (1936). *Nature* 138: 882–882.

**119** Wolf, K.L., Prahm, H., and Harms, H. (1937). *Z. Phys. Chem.* 36B: 237.

**120** Sidgwick, N.V. (1927). *Electronic Theory of Valency*. New York: Oxford University Press.

**121** Hine, J., Hahn, S., and Miles, D.E. (1986). *J. Org. Chem.* 51: 577–584.

**122** Hine, J. and Ahn, K. (1987). *J. Org. Chem.* 52: 2083–2086.

**123** Hine, J., Hahn, S., Miles, D.E., and Ahn, K. (1985). *J. Org. Chem.* 50: 5092–5096.

**124** Hine, J. and Ahn, K. (1987). *J. Org. Chem.* 52: 2089–2091.

**125** Kelly, T.R., Meghani, P., and Ekkundi, V.S. (1990). *Tetrahedron Lett.* 31: 3381–3384.

**126** Blake, J.F. and Jorgensen, W.L. (1991). *J. Am. Chem. Soc.* 113: 7430–7432.

**127** Blake, J.F., Lim, D., and Jorgensen, W.L. (1994). *J. Org. Chem.* 59: 803–805.

**128** Severance, D.L. and Jorgensen, W.L. (1992). *J. Am. Chem. Soc.* 114: 10966–10968.

**129** Etter, M.C. and Baures, P.W. (1988). *J. Am. Chem. Soc.* 110: 639–640.

**130** Etter, M.C. and Panunto, T.W. (1988). *J. Am. Chem. Soc.* 110: 5896–5897.
**131** Etter, M.C. and Reutzel, S.M. (1991). *J. Am. Chem. Soc.* 113: 2586–2598.
**132** Dannecker, W. and Kopf, J. (1979). *Acta Cryst.* 8: 429–432.
**133** Taylor, R. and Kennard, O. (1982). *J. Am. Chem. Soc.* 104: 5063–5070.
**134** Etter, M.C. (1991). *J. Phys. Chem. A* 95: 4601–4610.
**135** Smith, P.J., Reddington, M.V., and Wilcox, C.S. (1992). *Tetrahedron Lett.* 33: 6085–6088.
**136** Wilcox, C.S., Adrian, J.C. Jr.,, Webb, T.H., and Zawacki, F.J. (1992). *J. Am. Chem. Soc.* 114: 10189–10197.
**137** Wilcox, C.S., Kim, E.-i., Romano, D. *et al*. (1995). *Tetrahedron* 51: 621–634.
**138** Fan, E., Van Arman, S.A., Kincaid, S., and Hamilton, A.D. (1993). *J. Am. Chem. Soc.* 115: 369–370.
**139** Curran, D.P. and Kuo, L.H. (1995). *Tetrahedron Lett.* 36: 6647–6650.
**140** Curran, D.P. and Kuo, L.H. (1994). *J. Org. Chem.* 59: 3259–3261.
**141** Wittkopp, A. (1997). Wasserstoffbrückenbindungen als dirigierendeWechselwirkung in der organischen Synthese: Thioharnstoffe als Katalysatoren. Diploma Thesis. University of Göttingen, Germany.
**142** Kotke, M. and Schreiner, P.R. (2009). (Thio)urea Organocatalysts. In: *Hydrogen Bonding in Organic Synthesis* (ed. P.M. Pihko), 141–351. Weinheim: Wiley VCH.
**143** Jakab, G., Tancon, C., Zhang, Z. *et al*. (2012). *Org. Lett.* 14: 1724–1727.
**144** Busschaert, N., Karagiannidis, L.E., Wenzel, M. *et al*. (2014). *Chem. Sci.* 5: 1118–1127.
**145** Minami, T., Liu, Y., Akdeniz, A. *et al*. (2014). *J. Am. Chem. Soc.* 136: 11396–11401.
**146** Gómez, D.E., Fabbrizzi, L., Licchelli, M., and Monzani, E. (2005). *Org. Biomol. Chem.* 3: 1495–1500.
**147** Bonizzoni, M., Fabbrizzi, L., Taglietti, A., and Tiengo, F. (2006). *Eur. J. Org. Chem.* 2006: 3567–3574.
**148** Jiménez Blanco, J.L., Bootello, P., Benito, J.M. *et al*. (2006). *J. Org. Chem.* 71: 5136–5143.
**149** Custelcean, R. (2008). *Chem. Commun.* 44: 295–307.
**150** Succaw, G.L., Weakley, T.J.R., Han, F., and Doxsee, K.M. (2005). *Cryst. Growth Des.* 5: 2288–2298.
**151** Yonova, P.A. and Stoilkova, G.M. (2004). *J. Plant Growth Regul.* 23: 280–291.
**152** Richter, C.P. (1945). *JAMA* 129: 927–931.
**153** Bhogala, B.R., Captain, B., Parthasarathy, A., and Ramamurthy, V. (2010). *J. Am. Chem. Soc.* 132: 13434–13442.
**154** Harris, K.D.M. (1997). *Chem. Soc. Rev.* 26: 279–289.
**155** Harris, K.D.M. (2007). *Supramol. Chem.* 19: 47–53.
**156** Wittkopp, A. and Schreiner, P.R. (2000). *The Chemistry of Dienes and Polyenes*, vol. 2. New York: John Wiley & Sons.
**157** Wittkopp, A. and Schreiner, P.R. (2003). *Chem. Eur. J.* 9: 407–414.
**158** Schreiner, P.R. and Wittkopp, A. (2002). *Org. Lett.* 4: 217–220.
**159** Jai-Nhuknan, J., Karipides, A., Hughes, J., and Cantrell, J. (1997). *Acta Crystallogr. C* 53: 455–457.

**160** Kotke, M. (2010). Hydrogen-Bonding (Thio)urea Organocatalysts in Organic Synthesis: State of the Art and Practical Methods for Acetalization, Tetrahydropyranylation, and Cooperative Epoxide Alcoholysis. Dissertation, Universitätsbibliothek Gießen (University of Gießen, Germany, published online).
**161** Okino, T., Hoashi, Y., and Takemoto, Y. (2003). *J. Am. Chem. Soc.* 125: 12672–12673.
**162** Ooi, T., Miki, T., Taniguchi, M. *et al*. (2003). *Angew. Chem. Int. Ed.* 42: 3796–3798.
**163** Sohtome, Y., Tanatani, A., Hashimoto, Y., and Nagasawa, K. (2004). *Tetrahedron Lett.* 45: 5589–5592.
**164** Herrera, R.P., Sgarzani, V., Bernardi, L., and Ricci, A. (2005). *Angew. Chem. Int. Ed.* 44: 6576–6579.
**165** Honjo, T., Sano, S., Shiro, M., and Nagao, Y. (2005). *Angew. Chem. Int. Ed.* 44: 5838–5841.
**166** Wang, J., Li, H., Yu, X. *et al*. (2005). *Org. Lett.* 7: 4293–4296.
**167** Vakulya, B., Varga, S., Csámpai, A., and Soós, T. (2005). *Org. Lett.* 7: 1967–1969.
**168** Lan, Q., Wang, X., and Maruoka, K. (2007). *Tetrahedron Lett.* 48: 4675–4678.
**169** Klausen, R.S. and Jacobsen, E.N. (2009). *Org. Lett.* 11: 887–890.
**170** Zhang, Z., Lippert, K.M., Hausmann, H. *et al*. (2011). *J. Org. Chem.* 76: 9764–9776.
**171** Hayashi, Y., Gotoh, H., Hayashi, T., and Shoji, M. (2005). *Angew. Chem. Int. Ed.* 44: 4212–4215.
**172** Marigo, M., Wabnitz, T.C., Fielenbach, D., and Jørgensen, K.A. (2005). *Angew. Chem. Int. Ed.* 44: 794–797.
**173** Akiyama, T., Morita, H., Itoh, J., and Fuchibe, K. (2005). *Org. Lett.* 7: 2583–2585.
**174** Sigman, M.S. and Jacobsen, E.N. (1998). *J. Am. Chem. Soc.* 120: 4901–4902.
**175** Okino, T., Hoashi, Y., Furukawa, T. *et al*. (2005). *J. Am. Chem. Soc.* 127: 119–125.
**176** Kotke, M. and Schreiner, P.R. (2006). *Tetrahedron* 62: 434–439.
**177** Karimi, B., Hazarkhani, H., and Maleki, J. (2005). *Synthesis*: 279–285.
**178** Ranu, B.C., Jana, R., and Samanta, S. (2004). *Adv. Synth. Chem.* 346: 446–450.
**179** Mayr, H., Bug, T., Gotta, M.F. *et al*. (2001). *J. Am. Chem. Soc.* 123: 9500–9512.
**180** Tantillo, D.J. and Houk, K.N. (2002). *J. Comput. Chem.* 23: 84–95.
**181** Pauling, L. (1935). *J. Am. Chem. Soc.* 57: 2680–2684.
**182** Kotke, M. and Schreiner, P.R. (2007). *Synthesis* 2007: 779–790.
**183** Li, H., Wang, Y., Tang, L., and Deng, L. (2004). *J. Am. Chem. Soc.* 126: 9906–9907.
**184** Zuend, S.J. and Jacobsen, E.N. (2009). *J. Am. Chem. Soc.* 131: 15358–15374.
**185** Madarász, Á., Dósa, Z., Varga, S. *et al*. (2016). *ACS Catal.* 6: 4379–4387.
**186** Bradshaw, G.A., Colgan, A.C., Allen, N.P. *et al*. (2019). *Chem. Sci.* 10: 508–514.
**187** Balmond, E.I., Coe, D.M., Galan, M.C., and McGarrigle, E.M. (2012). *Angew. Chem. Int. Ed.* 51: 9152–9155.
**188** Rossini, E., Bochevarov, A.D., and Knapp, E.W. (2018). *ACS Omega* 3: 1653–1662.

**189** Hrdina, R., Müller, C.E., Wende, R.C. *et al*. (2011). *J. Am. Chem. Soc.* 133: 7624–7627.
**190** Lippert, K.M., Hof, K., Gerbig, D. *et al*. (2012). *Eur. J. Org. Chem.* 2012: 5919–5927.
**191** Malerich, J.P., Hagihara, K., and Rawal, V.H. (2008). *J. Am. Chem. Soc.* 130: 14416–14417.
**192** Alemán, J., Parra, A., Jiang, H., and Jørgensen, K.A. (2011). *Chem. Eur. J.* 17: 6890–6899.
**193** Chauhan, P., Mahajan, S., Kaya, U. *et al*. (2015). *Adv. Synth. Chem.* 357: 253–281.
**194** Storer, R.I., Aciro, C., and Jones, L.H. (2011). *Chem. Soc. Rev.* 40: 2330–2346.
**195** Ni, X., Li, X., Wang, Z., and Cheng, J.-P. (2014). *Org. Lett.* 16: 1786–1789.
**196** Prohens, R., Tomàs, S., Morey, J. *et al*. (1998). *Tetrahedron Lett.* 39: 1063–1066.
**197** Tomàs, S., Prohens, R., Vega, M. *et al*. (1996). *J. Org. Chem.* 61: 9394–9401.
**198** Davis, P.A., Draper, S., M., Dunne, G., and Ashton, P. (1999). *Chem. Commun.* 35: 2265–2266.
**199** Quiñonero, D., Prohens, R., Garau, C. *et al*. (2002). *Chem. Phys. Lett.* 351: 115–120.
**200** Zhao, B.-L., Li, J.-H., and Du, D.-M. (2017). *Chem. Rec.* 17: 994–1018.
**201** Rombola, M., Sumaria, C.S., Montgomery, T.D., and Rawal, V.H. (2017). *J. Am. Chem. Soc.* 139: 5297–5300.
**202** Busschaert, N., Elmes, R.B.P., Czech, D.D. *et al*. (2014). *Chem. Sci.* 5: 3617–3626.
**203** Elmes, R.B.P., Busschaert, N., Czech, D.D. *et al*. (2015). *Chem. Commun.* 51: 10107–10110.
**204** Ho, J., Zwicker, V.E., Yuen, K.K.Y., and Jolliffe, K.A. (2017). *J. Org. Chem.* 82: 10732–10736.
**205** Jeppesen, A., Nielsen, B.E., Larsen, D. *et al*. (2017). *Org. Biomol. Chem.* 15: 2784–2790.
**206** Zwicker, V.E., Yuen, K.K.Y., Smith, D.G. *et al*. (2018). *Chem. Eur. J.* 24: 1140–1150.
**207** Kumler, W.D. (1935). *J. Am. Chem. Soc.* 57: 600–605.
**208** Li, Y. and Flood, A.H. (2008). *Angew. Chem. Int. Ed.* 47: 2649–2652.
**209** Sutor, D.J. (1960). *Nature* 188: 47–48.
**210** Sutor, D.J. (1963). *Acta Crystallogr. A* 16: 97–104.
**211** Sutor, D.J. (1963). *J. Chem. Soc.*: 1105–1110.
**212** Zhu, S.S., Staats, H., Brandhorst, K. *et al*. (2008). *Angew. Chem. Int. Ed.* 47: 788–792.
**213** Li, Y. and Flood, A.H. (2008). *J. Am. Chem. Soc.* 130: 12111–12122.
**214** Juwarker, H., Lenhardt, J.M., Pham, D.M., and Craig, S.L. (2008). *Angew. Chem. Int. Ed.* 47: 3740–3743.
**215** Meudtner, R.M. and Hecht, S. (2008). *Angew. Chem. Int. Ed.* 47: 4926–4930.
**216** Yoon, D.-W., Gross, D.E., Lynch, V.M. *et al*. (2008). *Angew. Chem. Int. Ed.* 47: 5038–5042.
**217** Maeda, H., Mihashi, Y., and Haketa, Y. (2008). *Org. Lett.* 10: 3179–3182.

**218** Berryman, O.B., Sather, A.C., Hay, B.P. *et al*. (2008). *J. Am. Chem. Soc.* 130: 10895–10897.
**219** Nishio, M., Umezawa, Y., Fantini, J. *et al*. (2014). *Phys. Chem. Chem. Phys.* 16: 12648–12683.
**220** Desiraju, G.R. (1996). *Acc. Chem. Res.* 29: 441–449.
**221** Nishio, M., Umezawa, Y., Hirota, M., and Takeuchi, Y. (1995). *Tetrahedron* 51: 8665–8701.
**222** Nishio, M. (2004). *CrystEngComm* 6: 130–158.
**223** Nishio, M., Umezawa, Y., Honda, K. *et al*. (2009). *CrystEngComm* 11: 1757–1788.
**224** Takahashi, O., Kohno, Y., and Nishio, M. (2010). *Chem. Rev.* 110: 6049–6076.
**225** Nishio, M. (2011). *Phys. Chem. Chem. Phys.* 13: 13873–13900.
**226** Hua, Y. and Flood, A.H. (2010). *Chem. Soc. Rev.* 39: 1262–1271.
**227** McDonald, K.P., Hua, Y., Lee, S., and Flood, A.H. (2012). *Chem. Commun.* 48: 5065–5075.
**228** Zurro, M. and García Mancheño, O. (2017). *Chem. Rec.* 17: 485–498.
**229** Beckendorf, S., Asmus, S., Mück-Lichtenfeld, C., and García Mancheño, O. (2013). *Chem. Eur. J.* 19: 1581–1585.
**230** Asmus, S., Beckendorf, S., Zurro, M. *et al*. (2014). *Chem. Asian J.* 9: 2178–2186.
**231** Zurro, M., Asmus, S., Beckendorf, S. *et al*. (2014). *J. Am. Chem. Soc.* 136: 13999–14002.
**232** García Mancheño, O., Asmus, S., Zurro, M., and Fischer, T. (2015). *Angew. Chem. Int. Ed.* 54: 8823–8827.
**233** Fischer, T., Bamberger, J., and García Mancheño, O. (2016). *Org. Biomol. Chem.* 14: 5794–5802.
**234** Fischer, T., Duong, Q.-N., and García Mancheño, O. (2017). *Chem. Eur. J.* 23: 5983–5987.
**235** Duong, Q.-N., Schifferer, L., and García Mancheño, O. (2019). *Eur. J. Org. Chem.* 2019: 5452–5461.
**236** Zurro, M., Asmus, S., Bamberger, J. *et al*. (2016). *Chem. Eur. J.* 22: 3785–3793.
**237** Fischer, T., Bamberger, J., Gómez-Martínez, M. *et al*. (2019). *Angew. Chem. Int. Ed.* 58: 3217–3221.
**238** Eichstaedt, K., Jaramillo-Garcia, J., Leigh, D.A. *et al*. (2017). *J. Am. Chem. Soc.* 139: 9376–9381.
**239** Dorel, R. and Feringa, B.L. (2020). *Angew. Chem. Int. Ed.* 59: 785–789.
**240** Koumura, N., Zijlstra, R.W.J., van Delden, R.A. *et al*. (1999). *Nature* 401: 152–155.
**241** Lehnherr, D., Ford, D.D., Bendelsmith, A.J. *et al*. (2016). *Org. Lett.* 18: 3214–3217.
**242** Reisman, S.E., Doyle, A.G., and Jacobsen, E.N. (2008). *J. Am. Chem. Soc.* 130: 7198–7199.
**243** Wang, H., Wang, W., and Jin, W.J. (2016). *Chem. Rev.* 116: 5072–5104.
**244** Colin, M. (1814). *Ann. Chim.* 91: 252–272.
**245** Bineau, M.A. (1844). *C. R. Acad. Sci.* 55: 762–767.
**246** Guthrie, F. (1863). *J. Am. Chem. Soc.* 16: 239–244.

**247** Mulliken, R.S. (1950). *J. Am. Chem. Soc.* 72: 600–608.
**248** Mulliken, R.S. (1952). *J. Phys. Chem. A* 56: 801–822.
**249** Benesi, H.A. and Hildebrand, J.H. (1949). *J. Am. Chem. Soc.* 71: 2703–2707.
**250** Hassel, O. and Hvoslef, J. (1954). *Acta Chem. Scand.* 8: 873–873.
**251** Hassel, O. and Stromme, K. (1958). *Acta Chem. Scand.* 12: 1146–1147.
**252** Hassel, O. and Stromme, K. (1959). *Acta Chem. Scand.* 13: 1781–1786.
**253** Hassel, O. and Strømme, K. (1959). *Acta Chem. Scand.* 13: 275–280.
**254** Hassel, O. and Rømming, C. (1962). *Q. Rev. Chem. Soc.* 16: 1–18.
**255** Paolo, T.D. and Sandorfy, C. (1974). *Can. J. Chem.* 52: 3612–3622.
**256** Dumas, J.M., Peurichard, H., and Gomel, M. (1978). *J. Chem. Res.*: 54–55.
**257** Dumas, J.M., Gomel, M., and Guerin, M. (1983). Molecular Interactions Involving Organic Halides. In: *Halides, Pseudo-Halides and Azides* (eds. S. Patai and Z. Rappoport), 985–1020. Weinheim: Wiley VCH.
**258** Lim, J.Y.C. and Beer, P.D. (2018). *Chem* 4: 731–783.
**259** Clark, T. (2013). *WIREs Comput. Mol. Sci.* 3: 13–20.
**260** Bauzá, A. and Frontera, A. (2015). *Angew. Chem. Int. Ed.* 54: 7340–7343.
**261** Scholfield, M.R., Zanden, C.M.V., Carter, M., and Ho, P.S. (2013). *Protein Sci.* 22: 139–152.
**262** Politzer, P., Lane, P., Concha, M.C. *et al*. (2007). *J. Mol. Model.* 13: 305–311.
**263** Politzer, P. and Murray, J.S. (2013). *ChemPhysChem* 14: 278–294.
**264** Erdélyi, M. (2012). *Chem. Soc. Rev.* 41: 3547–3557.
**265** Wolters, L.P., Schyman, P., Pavan, M.J. *et al*. (2014). *WIREs Comput. Mol. Sci.* 4: 523–540.
**266** Beale, T.M., Chudzinski, M.G., Sarwar, M.G., and Taylor, M.S. (2013). *Chem. Soc. Rev.* 42: 1667–1680.
**267** Metrangolo, P., Neukirch, H., Pilati, T., and Resnati, G. (2005). *Acc. Chem. Res.* 38: 386–395.
**268** Clark, T., Hennemann, M., Murray, J.S., and Politzer, P. (2007). *J. Mol. Model.* 13: 291–296.
**269** Clark, T. (2017). *Faraday Discuss.* 203: 9–27.
**270** Politzer, P., Murray, J.S., Clark, T., and Resnati, G. (2017). *Phys. Chem. Chem. Phys.* 19: 32166–32178.
**271** Breugst, M. and Koenig, J.J. (2020). *Eur. J. Org. Chem.* 2020: 5473–5487.
**272** Walter, S.M., Kniep, F., Herdtweck, E., and Huber, S.M. (2011). *Angew. Chem. Int. Ed.* 50: 7187–7191.
**273** Walter, S.M., Kniep, F., Rout, L. *et al*. (2012). *J. Am. Chem. Soc.* 134: 8507–8512.
**274** Kniep, F., Jungbauer, S.H., Zhang, Q. *et al*. (2013). *Angew. Chem. Int. Ed.* 52: 7028–7032.
**275** Schottel, B.L., Chifotides, H.T., and Dunbar, K.R. (2008). *Chem. Soc. Rev.* 37: 68–83.
**276** Frontera, A., Gamez, P., Mascal, M. *et al*. (2011). *Angew. Chem. Int. Ed.* 50: 9564–9583.
**277** Frontera, A., Quiñonero, D., and Deyà, P.M. (2011). *WIREs Comput. Mol. Sci.* 1: 440–459.

**278** Quiñonero, D., Garau, C., Rotger, C. *et al*. (2002). *Angew. Chem. Int. Ed.* 41: 3389–3392.
**279** Alkorta, I., Rozas, I., and Elguero, J. (2002). *J. Am. Chem. Soc.* 124: 8593–8598.
**280** Mascal, M., Armstrong, A., and Bartberger, M.D. (2002). *J. Am. Chem. Soc.* 124: 6274–6276.
**281** Zhao, Y., Domoto, Y., Orentas, E. *et al*. (2013). *Angew. Chem. Int. Ed.* 52: 9940–9943.
**282** Zhao, Y., Beuchat, C., Domoto, Y. *et al*. (2014). *J. Am. Chem. Soc.* 136: 2101–2111.
**283** Lu, T. and Wheeler, S.E. (2014). *Org. Lett.* 16: 3268–3271.
**284** Zhao, Y., Cotelle, Y., Liu, L. *et al*. (2018). *Acc. Chem. Res.* 51: 2255–2263.
**285** Neel, A.J., Hilton, M.J., Sigman, M.S., and Toste, F.D. (2017). *Nature* 543: 637–646.
**286** Berkessel, A., Das, S., Pekel, D., and Neudörfl, J.-M. (2014). *Angew. Chem. Int. Ed.* 53: 11660–11664.
**287** Schafer, A.G., Wieting, J.M., Fisher, T.J., and Mattson, A.E. (2013). *Angew. Chem. Int. Ed.* 52: 11321–11324.
**288** Wieting, J.M., Fisher, T.J., Schafer, A.G. *et al*. (2015). *Eur. J. Org. Chem.* 2015: 525–533.
**289** Attard, J.W., Osawa, K., Guan, Y. *et al*. (2019). *Synthesis* 51: 2107–2115.
**290** Borovika, A., Tang, P.-I., Klapman, S., and Nagorny, P. (2013). *Angew. Chem. Int. Ed.* 52: 13424–13428.
**291** Weil, T., Kotke, M., Kleiner, C.M., and Schreiner, P.R. (2008). *Org. Lett.* 10: 1513–1516.
**292** Lee, J.H., Kim, W.H., and Danishefsky, S.J. (2010). *Tetrahedron Lett.* 51: 1252–1253.
**293** Wöhler, F. and v. Liebig, J. (1832). *Liebigs Ann.* 3: 249–282.
**294** Langenbeck, W. (1927). *Ber. Dtsch. Chem. Ges.* 60: 930–934.
**295** Langenbeck, W. (1928). *Angew. Chem.* 41: 740–745.
**296** Langenbeck, W. (1929). *Liebigs Ann.* 469: 16–25.
**297** Langenbeck, W. (1932). *Angew. Chem.* 45: 97–99.
**298** Langenbeck, W. (1949). *Die organischen Katalysatoren und ihre Beziehungen zu den Fermenten (Organic Catalysts and their Relation to the Enzymes)*. Berlin: Springer.
**299** Langenbeck, W. (1958). *Tetrahedron* 3: 185–196.
**300** v. Liebig, J. (1860). *Liebigs Ann.* 113: 246–247.
**301** v. Liebig, J. (1870). *Liebigs Ann.* 153: 1–47.
**302** Seebach, D. (1990). *Angew. Chem. Int. Ed.* 29: 1320–1367.
**303** Morrill, L.A., Susick, R.B., Chari, J.V., and Garg, N.K. (2019). *J. Am. Chem. Soc.* 141: 12423–12443.
**304** Simons, J.P. (1987). *J. Phys. Chem. A* 91: 5378–5387.
**305** Aldegunde, J., de Miranda, M.P., Haigh, J.M. *et al*. (2005). *J. Phys. Chem. A* 109: 6200–6217.
**306** Zhan, C.-G., Bentley, J., and Chipman, D.M. (1998). *J. Chem. Phys.* 108: 177–192.

**307** Ostwald, W. (1894). *Z. Phys. Chem.* 15: 705–707.
**308** Roberts, M.W. (2000). *Catal. Lett.* 67: 1–4.
**309** Palmer, T. and Bonner, P.L. (2011). The Chemical Nature of Enzyme Catalysis. In: *Enzymes*, 2e (eds. T. Palmer and P. L. Bonner), 189–221. Sawston: Horwood Publishing Ltd.
**310** List, B. (2007). *Chem. Rev.* 107: 5413–5883. special issue on organocatalysis.
**311** Abbasov, M.E. and Romo, D. (2014). *Nat. Prod. Rep.* 31: 1318–1327.
**312** Wende, R.C. and Schreiner, P.R. (2012). *Green Chem.* 14: 1821–1849.
**313** Seayad, J. and List, B. (2005). *Org. Biomol. Chem.* 3: 719–724.
**314** Berkessel, A. and Gröger, H. (2006). *Asymmetric Organocatalysis: From Biomimetic Concepts to Applications in Asymmetric Synthesis*. Weinheim: Wiley VCH.
**315** Marcia de Figueiredo, R. and Christmann, M. (2007). *Eur. J. Org. Chem.* 2007: 2575–2600.
**316** Marqués-López, E., Herrera, R.P., and Christmann, M. (2010). *Nat. Prod. Rep.* 27: 1138–1167.
**317** MacMillan, D.W.C. (2008). *Nature* 455: 304–308.
**318** Dalko, P.I. and Moisan, L. (2001). *Angew. Chem. Int. Ed.* 40: 3726–3748.
**319** Dalko, P.I. and Moisan, L. (2004). *Angew. Chem. Int. Ed.* 43: 5138–5175.
**320** Szwarc, M. (1969). *Acc. Chem. Res.* 2: 87–96.
**321** Bjerrum, N. (1926). *K. Dan. Vidensk. Selsk. Mat.-Fys. Medd.* 7: 3–48.
**322** Anslyn, E.V. and Dougherty, D.A. (2006). *Modern Physical Organic Chemistry*. Sausalito: University Science Books.
**323** Einstein, A. (1905). *Ann. Phys.* 322: 549–560.
**324** Marcus, Y. (1985). Solvation of Ion Pairs. In: *Ion Solvation* (ed. Y. Marcus), 218–244. Chichester: Wiley.
**325** Marcus, Y. and Hefter, G. (2006). *Chem. Rev.* 106: 4585–4621.
**326** Sadek, H. and Fuoss, R.M. (1954). *J. Am. Chem. Soc.* 76: 5897–5901.
**327** Winstein, S., Clippinger, E., Fainberg, A.H., and Robinson, G.C. (1954). *J. Am. Chem. Soc.* 76: 2597–2598.
**328** Erkkilä, A., Majander, I., and Pihko, P.M. (2007). *Chem. Rev.* 107: 5416–5470.
**329** Huang, Y., Walji, A.M., Larsen, C.H., and MacMillan, D.W.C. (2005). *J. Am. Chem. Soc.* 127: 15051–15053.
**330** Yamashita, Y., Yasukawa, T., Yoo, W.-J. *et al*. (2018). *Chem. Soc. Rev.* 47: 4388–4480.
**331** Romea, P. and Urpi, F. (2013). Stereoselective Acetate Aldol Reactions. In: *Modern Methods in Stereoselective Aldol Reactions* (ed. R. Mahrwald), 1–81. Weinheim: Wiley-VCH.
**332** Mayer, S. and List, B. (2006). *Angew. Chem. Int. Ed.* 45: 4193–4195.
**333** Corey, E.J. and Grogan, M.J. (1999). *Org. Lett.* 1: 157–160.
**334** Li, J., Jiang, W.-Y., Han, K.-L. *et al*. (2003). *J. Org. Chem.* 68: 8786–8789.
**335** Goerigk, L., Kruse, H., and Grimme, S. (2011). *ChemPhysChem* 12: 3421–3433.
**336** Wagner, J.P. and Schreiner, P.R. (2015). *Angew. Chem. Int. Ed.* 54: 12274–12296.
**337** Birrell, J.A., Desrosiers, J.-N., and Jacobsen, E.N. (2011). *J. Am. Chem. Soc.* 133: 13872–13875.

**338** Taylor, M.S. and Jacobsen, E.N. (2004). *J. Am. Chem. Soc.* 126: 10558–10559.
**339** Knowles, R.R., Lin, S., and Jacobsen, E.N. (2010). *J. Am. Chem. Soc.* 132: 5030–5032.
**340** Kutateladze, D.A., Strassfeld, D.A., and Jacobsen, E.N. (2020). *J. Am. Chem. Soc.* 142: 6951–6956.
**341** Seidel, D. (2014). *Synlett* 25: 783–794.
**342** De, C.K., Klauber, E.G., and Seidel, D. (2009). *J. Am. Chem. Soc.* 131: 17060–17061.
**343** De, C.K., Mittal, N., and Seidel, D. (2011). *J. Am. Chem. Soc.* 133: 16802–16805.
**344** Banik, S.M., Levina, A., Hyde, A.M., and Jacobsen, E.N. (2017). *Science* 358: 761–764.
**345** Wendlandt, A.E., Vangal, P., and Jacobsen, E.N. (2018). *Nature* 556: 447–451.
**346** Pupo, G., Ibba, F., Ascough, D.M.H. *et al.* (2018). *Science* 360: 638–642.
**347** Roagna, G., Ascough, D.M.H., Ibba, F. *et al.* (2020). *J. Am. Chem. Soc.* 142: 14045–14051.
**348** Pupo, G., Vicini, A.C., Ascough, D.M.H. *et al.* (2019). *J. Am. Chem. Soc.* 141: 2878–2883.
**349** Sigman, M.S., Vachal, P., and Jacobsen, E.N. (2000). *Angew. Chem. Int. Ed.* 39: 1279–1281.
**350** HCN was generated by the method of Ziegler. Alternatively, generation of HCN in situ by reaction of TMSCN and MeOH afforded identical results: Ziegler, K. (1932). In: *Organic Syntheses Collective*, Volume 1 (eds. H. Gilman and H. Blatt), p. 314. New York: Wiley
**351** Vachal, P. and Jacobsen, E.N. (2002). *J. Am. Chem. Soc.* 124: 10012–10014.
**352** Wittkopp, A. (2001). Organokatalyse von Diels–Alder-Reaktionen durch neutrale Wasserstoffbrückendonoren in organischen und wässrigen Lösungsmitteln. Dissertation, University of Göttingen, Germany, published online (Germany).
**353** Tárkányi, G., Király, P., Varga, S. *et al.* (2008). *Chem. Eur. J.* 14: 6078–6086.
**354** Oh, S.H., Rho, H.S., Lee, J.W. *et al.* (2008). *Angew. Chem. Int. Ed.* 47: 7872–7875.
**355** Zuend, S.J., Coughlin, M.P., Lalonde, M.P., and Jacobsen, E.N. (2009). *Nature* 461: 968–970.
**356** Wadhwa, P., Kharbanda, A., and Sharma, A. (2018). *Asian J. Org. Chem.* 7: 634–661.
**357** Enders, D., Lüttgen, K., and Narine, A.A. (2007). *Synthesis* 2007: 959–980.
**358** Enders, D., Wang, C., and Liebich, J.X. (2009). *Chem. Eur. J.* 15: 11058–11076.
**359** Zhu, R., Zhang, D., Wu, J., and Liu, C. (2006). *Tetrahedron: Asymmetry* 17: 1611–1616.
**360** Hoashi, Y., Yabuta, T., and Takemoto, Y. (2004). *Tetrahedron Lett.* 45: 9185–9188.
**361** Hoashi, Y., Yabuta, T., Yuan, P. *et al.* (2006). *Tetrahedron* 62: 365–374.
**362** Takemoto, Y. (2010). *Chem. Pharm. Bull.* 58: 593–601.
**363** An overview of numerous application is discussed in Kotke, M., Schreiner, P. R. (2009). (Thio)urea Organocatalysts. In: *Hydrogen Bonding in Organic Synthesis* (ed. P. M. Pihko), 141–351. Weinheim: Wiley VCH.

**364** Hamza, A., Schubert, G., Soós, T., and Pápai, I. (2006). *J. Am. Chem. Soc.* 128: 13151–13160.
**365** Izzo, J.A., Myshchuk, Y., Hirschi, J.S., and Vetticatt, M.J. (2019). *Org. Biomol. Chem.* 17: 3934–3939.
**366** Tan, B., Lu, Y., Zeng, X. *et al*. (2010). *Org. Lett.* 12: 2682–2685.
**367** Nishizawa, S., Bühlmann, P., Iwao, M., and Umezawa, Y. (1995). *Tetrahedron Lett.* 36: 6483–6486.
**368** Wenzel, A.G. and Jacobsen, E.N. (2002). *J. Am. Chem. Soc.* 124: 12964–12965.
**369** Bentley, K.W. (2004). *Nat. Prod. Rep.* 21: 395–424.
**370** Bentley, K.W. (2006). *Nat. Prod. Rep.* 23: 444–463.
**371** Taylor, M.S., Tokunaga, N., and Jacobsen, E.N. (2005). *Angew. Chem. Int. Ed.* 44: 6700–6704.
**372** Bose, A.K., Spiegelman, G., and Manhas, M.S. (1971). *Tetrahedron Lett.* 12: 3167–3170.
**373** Raheem, I.T., Thiara, P.S., Peterson, E.A., and Jacobsen, E.N. (2007). *J. Am. Chem. Soc.* 129: 13404–13405.
**374** Dijkink, J. and Speckamp, W.N. (1977). *Tetrahedron Lett.* 18: 935–938.
**375** Dijkink, J. and Speckamp, W.N. (1978). *Tetrahedron* 34: 173–178.
**376** Ford, D.D., Lehnherr, D., Kennedy, C.R., and Jacobsen, E.N. (2016). *J. Am. Chem. Soc.* 138: 7860–7863.
**377** Ford, D.D., Lehnherr, D., Kennedy, C.R., and Jacobsen, E.N. (2016). *ACS Catal.* 6: 4616–4620.
**378** Kennedy, C.R., Lehnherr, D., Rajapaksa, N.S. *et al*. (2016). *J. Am. Chem. Soc.* 138: 13525–13528.
**379** Park, Y., Harper, K.C., Kuhl, N. *et al*. (2017). *Science* 355: 162–166.
**380** Lairson, L.L., Henrissat, B., Davies, G.J., and Withers, S.G. (2008). *Annu. Rev. Biochem.* 77: 521–555.
**381** Nigudkar, S.S. and Demchenko, A.V. (2015). *Chem. Sci.* 6: 2687–2704.
**382** Albert, J.S. and Hamilton, A.D. (1993). *Tetrahedron Lett.* 34: 7363–7366.
**383** Kelly, T.R. and Kim, M.H. (1994). *J. Am. Chem. Soc.* 116: 7072–7080.
**384** Boiocchi, M., Del Boca, L., Gómez, D.E. *et al*. (2004). *J. Am. Chem. Soc.* 126: 16507–16514.
**385** Amendola, V., Esteban-Gómez, D., Fabbrizzi, L., and Licchelli, M. (2006). *Acc. Chem. Res.* 39: 343–353.
**386** Lee, Y., Klausen, R.S., and Jacobsen, E.N. (2011). *Org. Lett.* 13: 5564–5567.
**387** Klausen, R.S., Kennedy, C.R., Hyde, A.M., and Jacobsen, E.N. (2017). *J. Am. Chem. Soc.* 139: 12299–12309.
**388** Burns, N.Z., Witten, M.R., and Jacobsen, E.N. (2011). *J. Am. Chem. Soc.* 133: 14578–14581.
**389** Klauber, E.G., De, C.K., Shah, T.K., and Seidel, D. (2010). *J. Am. Chem. Soc.* 132: 13624–13626.
**390** Klauber, E.G., Mittal, N., Shah, T.K., and Seidel, D. (2011). *Org. Lett.* 13: 2464–2467.
**391** Min, C., Mittal, N., De, C.K., and Seidel, D. (2012). *Chem. Commun.* 48: 10853–10855.
**392** Mittal, N., Sun, D.X., and Seidel, D. (2012). *Org. Lett.* 14: 3084–3087.

**393** Mittal, N., Lippert, K.M., De, C.K. *et al.* (2015). *J. Am. Chem. Soc.* 137: 5748–5758.

**394** Lutz, V., Glatthaar, J., Würtele, C. *et al.* (2009). *Chem. Eur. J.* 15: 8548–8557.

**395** Wang, Z.-X., Tu, Y., Frohn, M. *et al.* (1997). *J. Am. Chem. Soc.* 119: 11224–11235.

**396** Kagan, H. and Fiaud, J. (1988). *Top. Stereochem.* 18: 21.

**397** Müller, K., Faeh, C., and Diederich, F. (2007). *Science* 317: 1881–1886.

**398** Purser, S., Moore, P.R., Swallow, S., and Gouverneur, V. (2008). *Chem. Soc. Rev.* 37: 320–330.

**399** Ojima, I. (2009). *Fluorine in Medicinal Chemistry and Chemical Biology*. New York: John Wiley & Sons.

**400** Gouverneur, V. and Müller, K. (2012). *Fluorine in Pharmaceutical and Medicinal Chemistry: From Biophysical Aspects to Clinical Applications*. Singapur: World Scientific.

**401** Jeschke, P. (2004). *ChemBioChem* 5: 570–589.

**402** Gillis, E.P., Eastman, K.J., Hill, M.D. *et al.* (2015). *J. Med. Chem.* 58: 8315–8359.

**403** Nelson, A. (1999). *Angew. Chem. Int. Ed.* 38: 1583–1585.

**404** Ooi, T. and Maruoka, K. (2007). *Angew. Chem. Int. Ed.* 46: 4222–4266.

**405** Maruoka, K. (2008). *Asymmetric Phase Transfer Catalysis*. Weinheim: Wiley VCH.

**406** Esteban-Gómez, D., Fabbrizzi, L., and Licchelli, M. (2005). *J. Org. Chem.* 70: 5717–5720.

**407** Jose, D.A., Kumar, D.K., Ganguly, B., and Das, A. (2004). *Org. Lett.* 6: 3445–3448.

**408** Pfeifer, L., Engle, K.M., Pidgeon, G.W. *et al.* (2016). *J. Am. Chem. Soc.* 138: 13314–13325.

**409** Yang, X., Wu, T., Phipps, R.J., and Toste, F.D. (2015). *Chem. Rev.* 115: 826–870.

**410** Auria-Luna, F., Mohammadi, S., Divar, M. *et al.* (2020). *Adv. Synth. Chem.* 362: 5275–5300.

**411** Nyffeler, P.T., Durón, S.G., Burkart, M.D. *et al.* (2005). *Angew. Chem. Int. Ed.* 44: 192–212.

**412** Wang, X., Lan, Q., Shirakawa, S., and Maruoka, K. (2010). *Chem. Commun.* 46: 321–323.

**413** Rauniyar, V., Lackner, A.D., Hamilton, G.L., and Toste, F.D. (2011). *Science* 334: 1681–1684.

**414** O'Hagan, D., Schaffrath, C., Cobb, S.L. *et al.* (2002). *Nature* 416: 279–279.

**415** Zhu, X., Robinson, D.A., McEwan, A.R. *et al.* (2007). *J. Am. Chem. Soc.* 129: 14597–14604.

**416** O'Hagan, D. and Deng, H. (2015). *Chem. Rev.* 115: 634–649.

**417** Morgenthaler, M., Schweizer, E., Hoffmann-Röder, A. *et al.* (2007). *ChemMedChem* 2: 1100–1115.

**418** Briggs, C.R.S., O'Hagan, D., Howard, J.A.K., and Yufit, D.S. (2003). *J. Fluor. Chem.* 119: 9–13.

**419** Sofia, M.J., Bao, D., Chang, W. *et al.* (2010). *J. Med. Chem.* 53: 7202–7218.

**420** Sato, K., Hoshino, K., Tanaka, M. *et al.* (1992). *Antimicrob. Agents Chemother.* 36: 1491–1498.